V.2. Accuracy and Reliability of Endoanal Ultrasonography in the Evaluation of Perianal Abscesses and Fistula-in-ano

G.A. Santoro, C. Ratto

The configuration of perianal sepsis and the relationship of abscesses or fistulas with internal and external sphincters are most important factors influencing the results of surgical management [1]. Preoperative identification of all loculate purulent areas and definition of the anatomy of the primary fistulous tract, secondary extensions, and the internal opening plays an important role in adequate planning of the operative approach in order to ensure complete drainage of abscesses, to prevent early recurrence after surgical treatment, and to minimize iatrogenic damage of sphincters and the risk of minor or major degrees of incontinence. It has been suggested that detailed knowledge of fistula characteristics may allow a reduction in the occurrence of both these adverse events [2]. Clinical evaluation, including fistula probing, has severe limitations on account of poor reliability in detecting the location of the internal opening and the possible existence of secondary tracts [3–7]. On the other hand, fistulography, traditionally adopted in the diagnostic workup, has been shown to be of poor accuracy in correlating the tract route with the local anatomic musculature and spaces [2–3, 8–9].

Over the last two decades, endoanal ultrasonography (EAUS) has been demonstrated to be a very helpful diagnostic tool, showing interesting features in accurately assessing all fistula or abscess characteristics [4–6, 9–13]. EAUS can be easily repeated while following patients with perianal sepsis to choose the optimal timing and modality of surgical treatment, to evaluate integrity or damage of sphincters after operation, and to identify fistula recurrence. EAUS still has some limitations and requires experience, but it is a rapid, simple, and well-tolerated technique. It also gives information about the state of the anal sphincters, which is valuable in performing successful fistula surgery. A fistula tract affecting minimal muscle can be safely excised, but where the bulk of external sphincter muscle is affected, it is best treated by seton drainage or mucosal advancement flap [1]. However, EAUS does not provide an adequate deep and global display of all adjacent pelvic and perineal spaces that may be involved.

The addition of hydrogen peroxide injection through the external opening of the fistula appears to improve the diagnostic accuracy of standard EAUS; where it is injected, hydrogen peroxide produces a significant increase in the echogenicity of the fistulous tract, which then appears as hyperechoic instead of hypoechoic. This method of hydrogen-peroxide-enhanced ultrasonography (HPUS) can thus be helpful in identifying tracts that had not been observed at the standard EAUS examination or the presence of which had not been definitively established [14, 15]. It can be also particularly useful when an active fistulous tract needs to be distinguished from postsurgical or posttrauma scar tissue that can cause tissue alterations that are difficult to analyze [15]. Moreover, HPUS has proven superior

to conventional EAUS in the assessment and classification of fistula-in-ano in patients with Crohn's disease [16].

A new technique is three-dimensional (3-D) EAUS, which enables reconstruction of transversal images of the anal canal in the coronal and sagittal planes. The use of 3-D EAUS might be very helpful in tracing the pathway of a tract and should be able to provide a significant contribution by increasing accuracy. *Volume render mode* is a special feature that successfully can be applied to high-resolution 3-D data volumes. Imaging processing includes maximum intensity, minimum intensity, and summed voxel projections, combined with positional or intensity weighting. This technique changes the depth information of 3-D data volume so information inside the cube to some extent is reconstructed.

Endoanal Ultrasonography Findings

The ultrasound examination is generally started using 10 MHz, changing to 7 or 5 MHz to optimize visualization of the deeper structures external to the anal sphincters. The puborectalis muscle and external, longitudinal, and internal sphincters should always be identified and used as referents for the spatial orientation of the fistula or abscess.

An anal abscess appears as a hypoechoic dishomogeneous area, sometimes with hyperechoic spots within it, possibly in connection with a fistulous tract directed through the anal canal lumen. Infection can spread in a number of directions, usually along the path of least resistance (Fig. V.17). Abscesses are classified as superficial (Fig. V.18), intersphincteric (Fig. V.19), ischiorectal (Fig. V.20), supralevator (Fig. V.21), pelvirectal (Fig. V.22), and horseshoe (Fig. V.23).

An anal fistula appears as a hypoechoic tract, which is followed along its crossing of the subepithelium, internal or external sphincters, and through the perianal spaces. With regard to the anal sphincters, according to the classification by Parks et al. [3], the fistulous primary tract can be classified into four types:

1. Intersphincteric tract, which is presented as a band of poor reflectivity within the longitudinal layer, causing widening and distortion of an otherwise narrow intersphincteric plane (Figs. V.24 and 25). The tract goes through the intersphincteric space without traversing the external sphincter fibers
2. Transsphincteric tract, in which the extension through the external sphincter is clearly shown by a poorly reflective tract running out through the external sphincter and disrupting its normal architecture (Fig. V.26). The point at which the main tract of the fistula traverses the sphincters defines the fistula level. The transsphincteric fistulas are divided into high, medium, or low, corresponding to the ultrasound level of the anal canal. The low

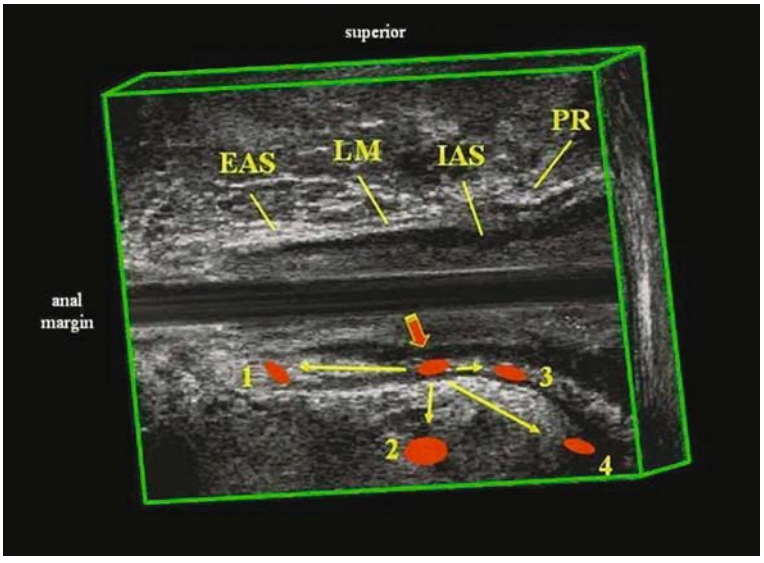

Fig. V.17. Sagittal view from a three-dimensional data set. Infection of the anal gland at the level of the dentate line (*arrow*) can spread superficially (*1*) or in the ischioanal (*2*), intersphincteric (*3*), or suprasphincteric (*4*) spaces. *EAS* external anal sphincter, *LM* longitudinal muscle, *IAS* internal anal sphincter, *PR* puborectalis muscle

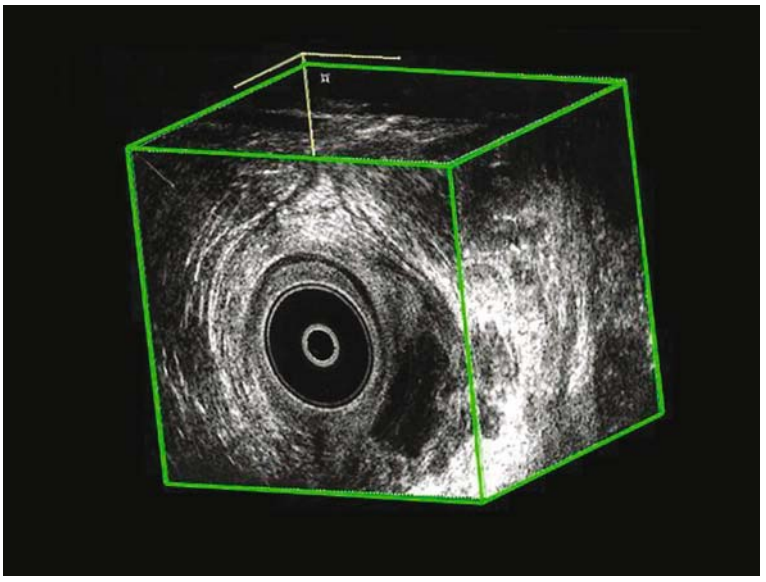

Fig. V.18. Acute superficial abscess presenting as an area of low reflectivity in the left side of the anal canal below the level of the internal sphincter

transsphincteric tract traverses only the distal third of the external sphincter at the lower portion of the medium anal canal (Fig. V.27). The medium transsphincteric tract traverses both sphincters, external and internal, in the middle part of the medium anal canal (Fig. V.28). The high transsphincteric tract traverses both sphincters in the higher part of the medium anal canal in the space below the puborectalis muscle (Fig. V.29)

3. Suprasphincteric tract, which goes above or through the puborectalis level (Fig. V.30). To detect supralevator extension, it is often necessary to fit the rectal balloon system to make contact with the distal rectal wall
4. Extrasphincteric tract, which may be seen close to but more laterally placed around the external sphincter (Fig. V.31).

Differentiation between granulated tracts and scars is sometimes difficult. Straight tracts are easily identified, but smaller and oblique tracts are more difficult to image. Secondary tracts, when present, are related to the main one and are

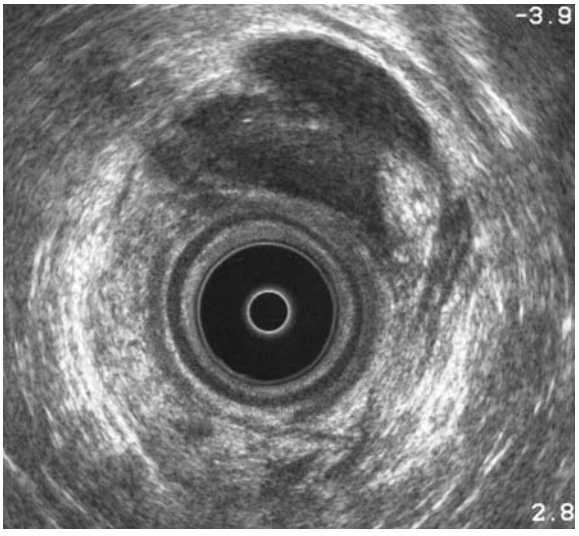

Fig. V.19. Acute intersphincteric abscess presenting as an area of low reflectivity in the anterior intersphincteric space

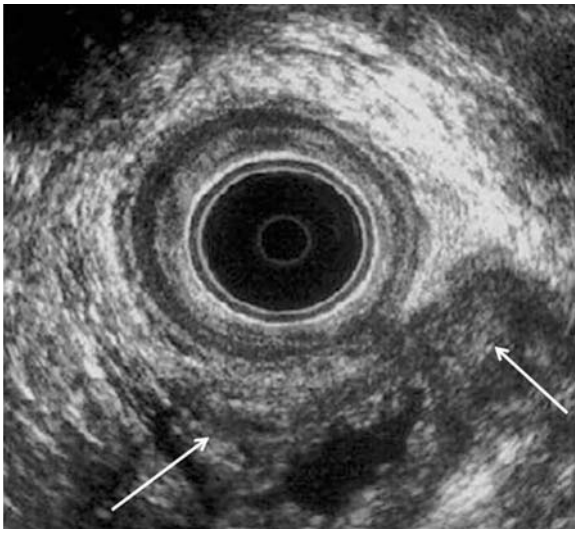

Fig. V.20. Acute abscess in the deep posterior ischioanal space (*arrows*)

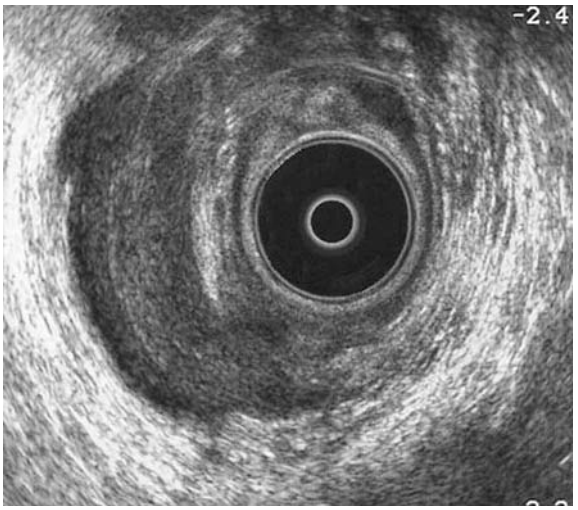

a

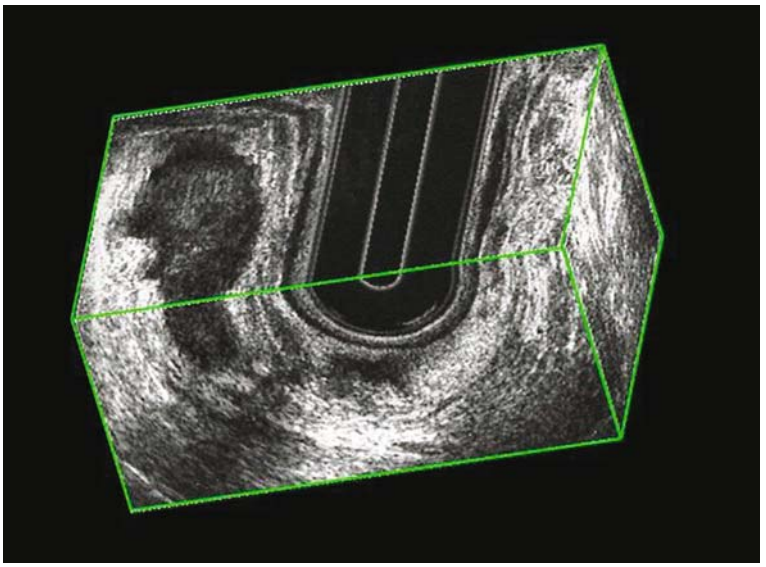

b

Fig. V.21. Acute supralevator abscess presenting as an area of low reflectivity in the right side of the anal canal deep beyond the puborectalis muscle (**a**). Coronal view from a three-dimensional data set (**b**). The longitudinal extension of the collection is more easily appreciated

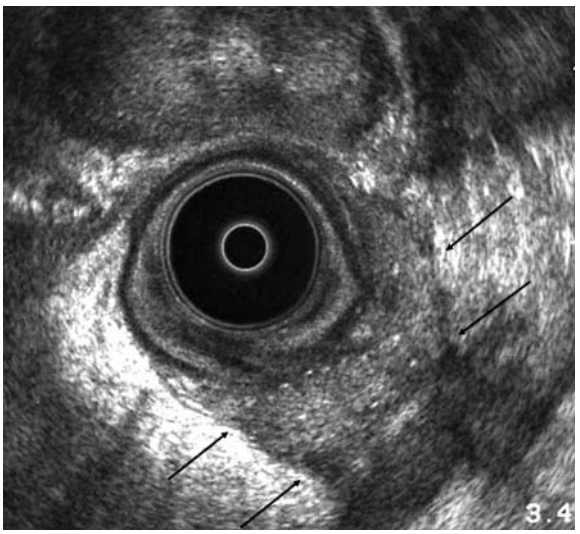

Fig. V.22. Pelvirectal abscess (*arrows*) at the prostate level, developed for a dehiscence of a colorectal anastomosis for rectal cancer

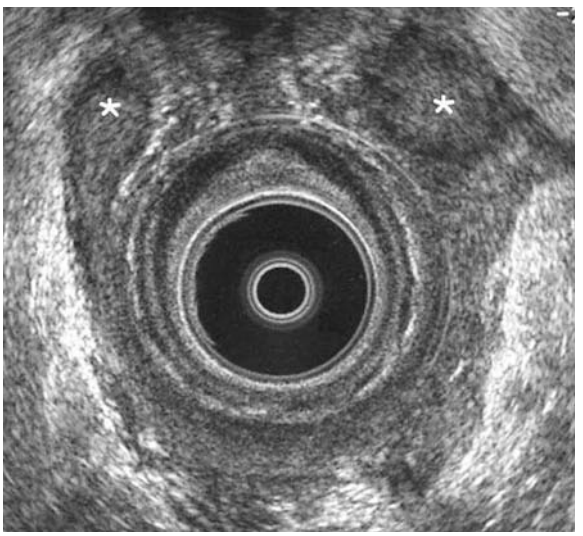

Fig. V.23. Horseshoe collection in the supralevator space

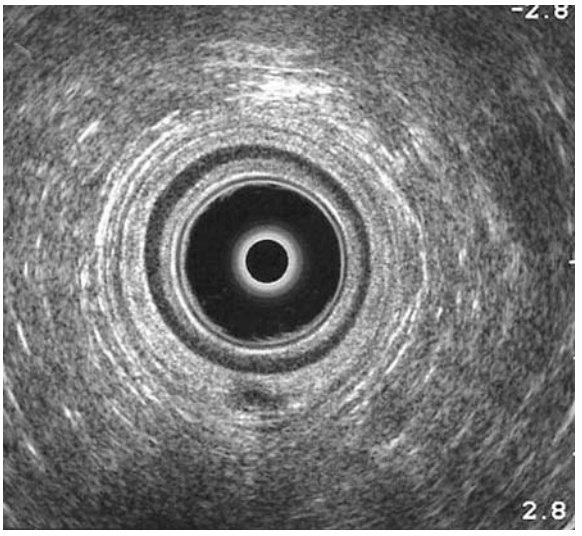

Fig. V.24. Posterior intersphincteric fistula at 6 o'clock

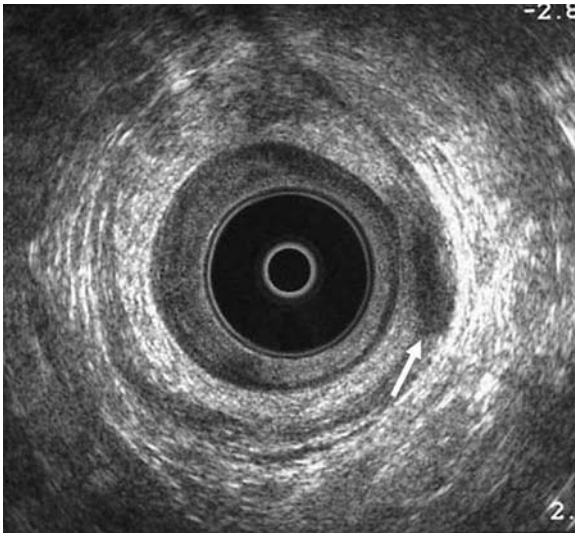

a

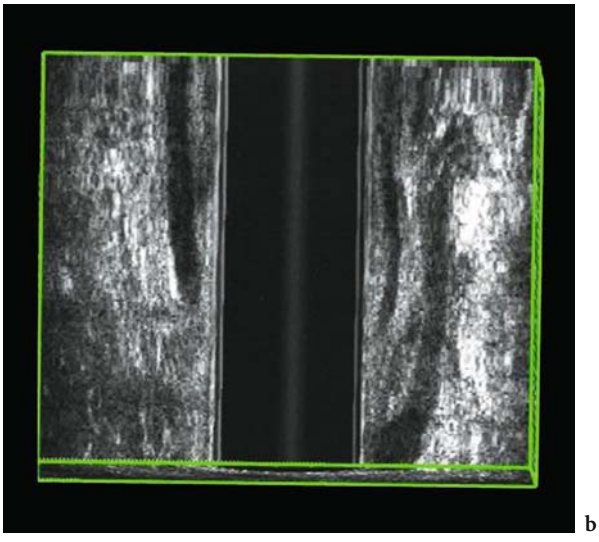

b

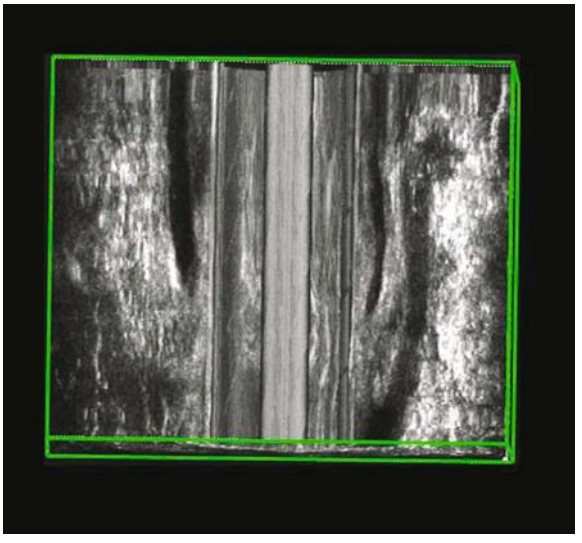

c

Fig. V.25. Axial endosonographic image of mid anal canal level. A hypoechoic area in the intersphincteric space is present at 3 o'clock (*arrow*) (**a**). Three-dimensional reconstruction in the coronal plane confirms an intersphincteric tract, appearing as a band of poor reflectivity within the plane, causing widening and distortion of an otherwise narrow plane. The tract extends through the intersphincteric space without traversing the external sphincter fibers (**b**). Volume render mode of the same image as in b (**c**)

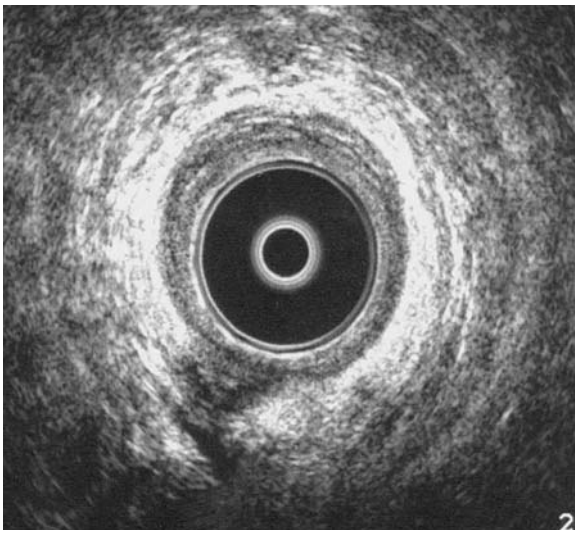

Fig. V.26. Posterior transsphincteric tract extending through the external sphincter

classified as intersphincteric, transsphincteric, suprasphincteric, or extrasphincteric (Fig. V.32). Similarly, horseshoe tracts, when identified, are categorized as intersphincteric, suprasphincteric, or extrasphincteric (Fig. V.33).

The dentate line is not visible as an anatomical structure but is assumed to be just below the midpoint of the internal sphincter. For this reason, the internal opening of an anal fistula is seldom clearly defined.

Endosonographic criteria for the site of an internal opening, according to Cho [17], are the following:

1. An appearance of a root-like budding formed by the intersphincteric tract, which contacts the internal anal sphincter (IAS) (Fig. V.34)
2. An appearance of a root-like budding with an IAS defect (Fig. V.35)
3. A subepithelial breach connecting to the intersphincteric tract through an IAS defect (Fig. V.36).

The site is categorized as being above, at, or below the dentate line (in relation to the presumed location of the dentate line at the middle third of the anal canal) or in the rectal ampulla. In addition, the site of the internal opening can also be characterized by the clock position, being classified from 1 to 12 o'clock. The internal opening can be identified as hypoechoic (when acute inflammation is present) or hyperechoic (when chronically inflamed).

After standard EAUS examination, in patients in whom the external fistula opening is patent, 1.0–2.0 ml of 3% hydrogen peroxide can be injected very slowly using an 18-gauge plastic cannula via this opening while ultrasonic scanning of the anal canal is performed [18]. When no obvious external opening is present, a focal, elevated, erythematous region immediately adjacent to the

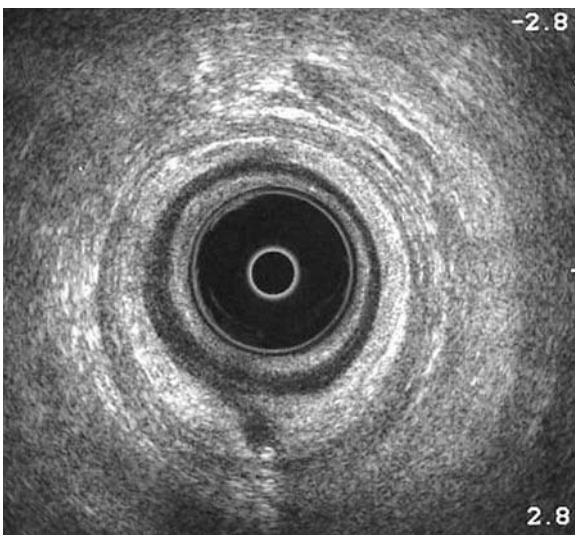

a

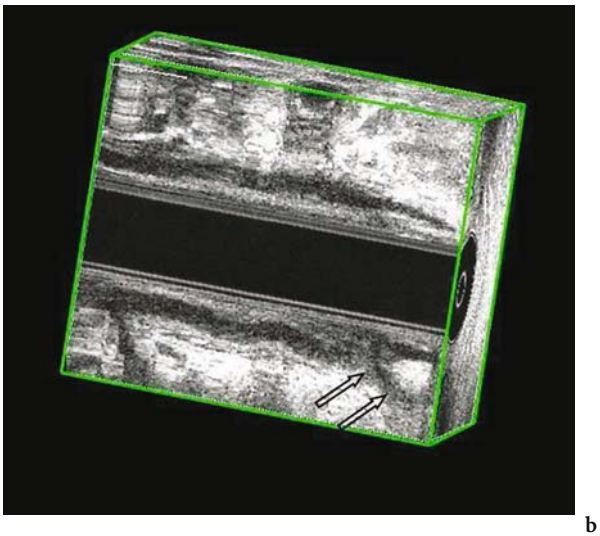

b

Fig. V.27. Low transsphincteric fistula at 6 o'clock (**a**). Sagittal view from a three-dimensional data set confirming that the tract (*arrows*) traverses only the distal third of the external sphincter at the lower portion of the medium anal canal (**b**)

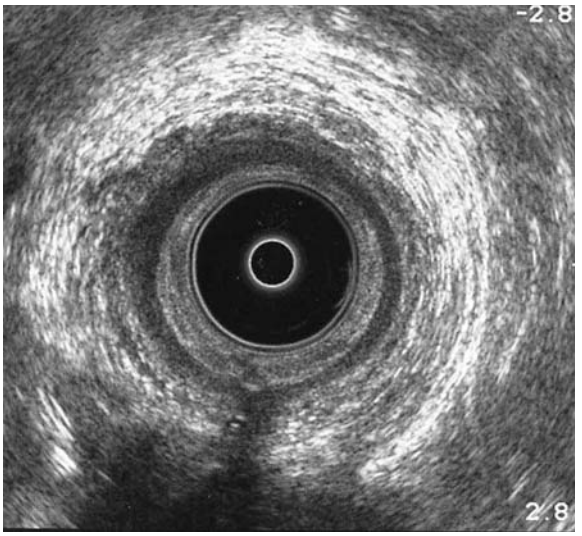

a

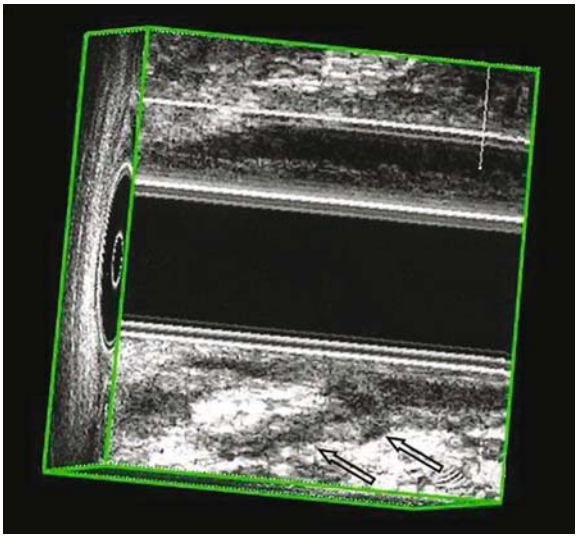

b

Fig. V.28. Medium transsphincteric fistula at 6 o'clock (**a**). Sagittal view from a three-dimensional data set confirming that the tract (*arrows*) traverses the middle part of the external sphincter (**b**)

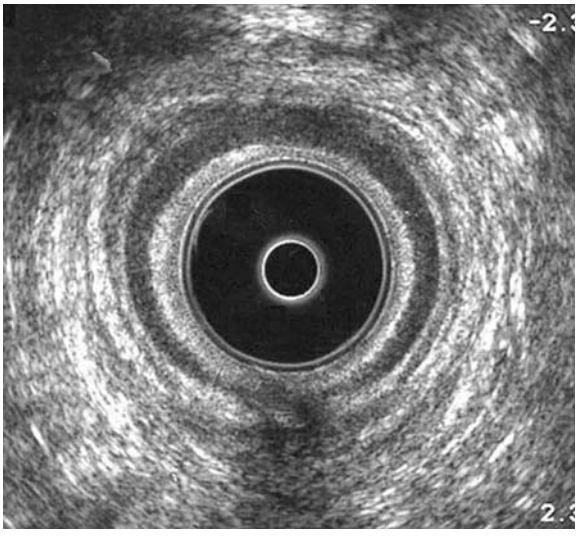

Fig. V.29. High transsphincteric tract traversing both sphincters in the higher part of the medium anal canal in the space below the puborectalis

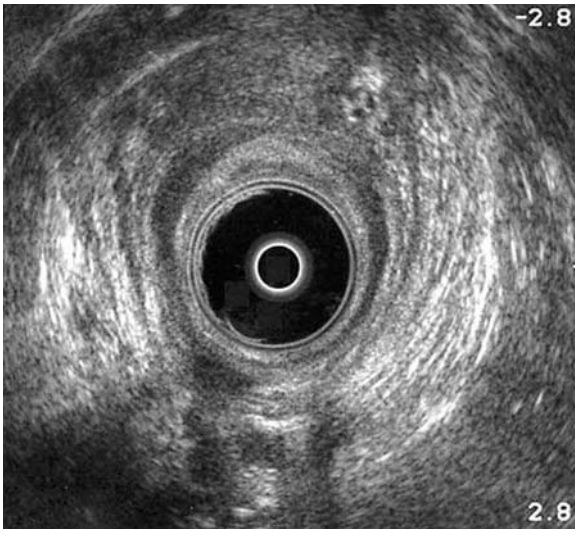

Fig. V.30. Suprasphincteric tract extending through the puborectalis muscle

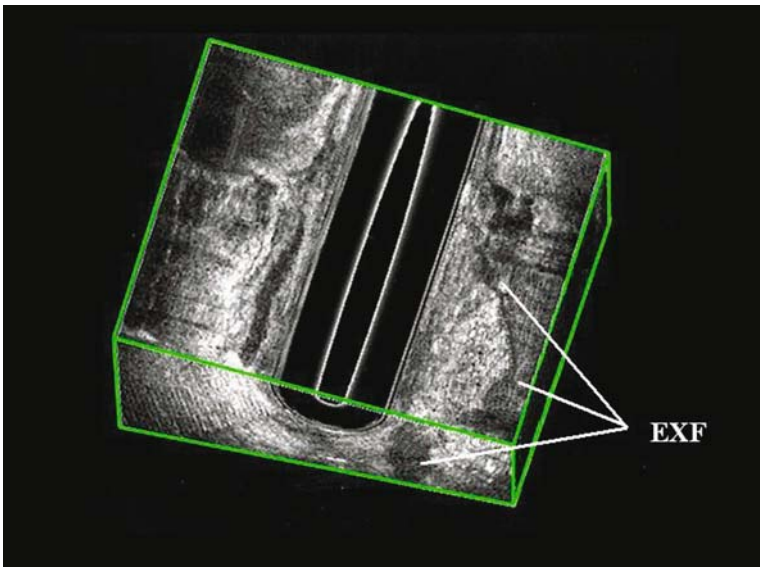

Fig. V.31. Extrasphincteric fistula (*EXF*) with direct communication between the perineum and rectum and no anal canal involvement

anal orifice is frequently identified. The soft catheter tip should be firmly pressed onto or probed into the center of this region, where the skin is easily broken, and the external opening located. Gas is a strong ultrasound reflector, and after injection fistula tracks become hyperechoic, and the internal opening is identified as an echogenic breach at the submucosa (Fig. V.37). According to Navarro-Luna et al. [19], injection should be performed in two phases: an initial injection of a small amount of hydrogen peroxide and a further injection at a greater pressure to determine whether there are secondary tracts that initially might be undetected [19]. During this technique, however, the operator must be careful because the injected hydrogen peroxide often results in bubbling into the anal canal, which then acts as a barrier to the ultrasound wave. Another disadvantage inherent to hydrogen peroxide injection is the very strong reflection that occurs at a gas/tissue interface, which blanks out any detail deep beyond this interface. The bubbles produced by hydrogen peroxide induce acoustic shadowing deep beyond the tract, so all information deep beyond the inner surface of the tract is lost (Fig. V.38). To reduce this potential pitfall of imaging, a volume-rendered 3-D data set can facilitate the following of a tortuous fistula tract due to the transparency and depth information (Fig. V.39).

Accuracy and Reliability

EAUS is able to identify the echo structure of the anal sphincters and allow the accurate identification of perianal sepsis. An early report [10] from St. Mark's Hospital, London, described the good tolerability of this procedure and its accuracy for the selective identification of fistula and abscess configurations. Primary tracts were correctly detected in 91.7% of patients and perianal abscesses in 75% of patients. In that study, a significant number of internal openings (33.3%) was not identified by use of a break in the mucosal layer as endosonographic criterion, possibly because of the proximity of the mucosa to the probe so that it was not within focal range. Subsequently, Seow-Choen et al. [5] underlined the high accuracy of EAUS in detecting a large proportion of internal openings, intersphincteric, and transsphincteric tracts. They described revised ultrasonographic criteria for identifying an internal opening, which included one or more of the following features: a hypoechoic breach of the subepithelial layer of the anorectum, a defect in the circular muscles of the internal anal sphincter, and a hypoechoic lesion of the normally hyperechoic longitudinal muscle abutting on the normally hypoechoic circular smooth muscle. In spite of the improvement in accuracy (73%), their results revealed no significant differ-

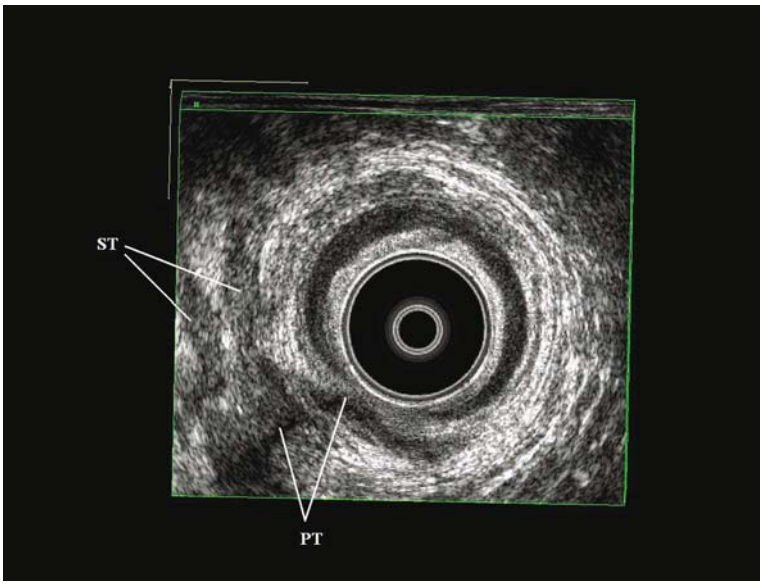

a

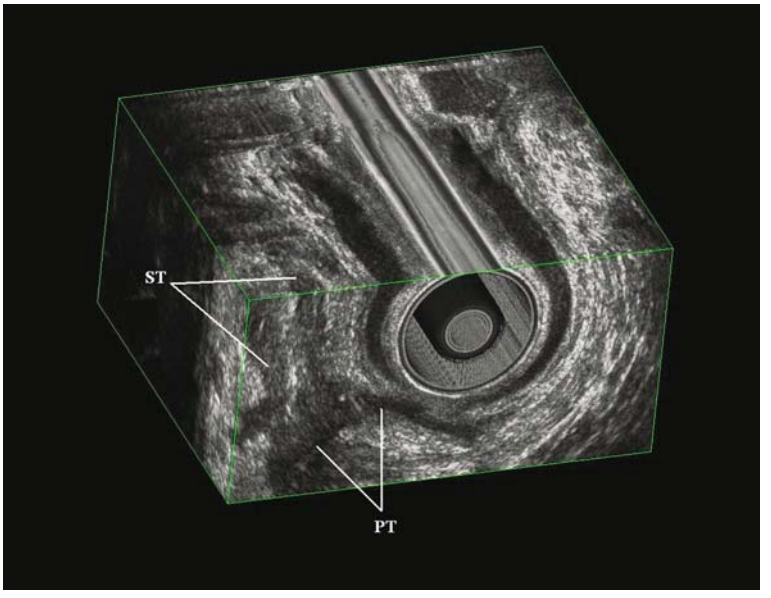

b

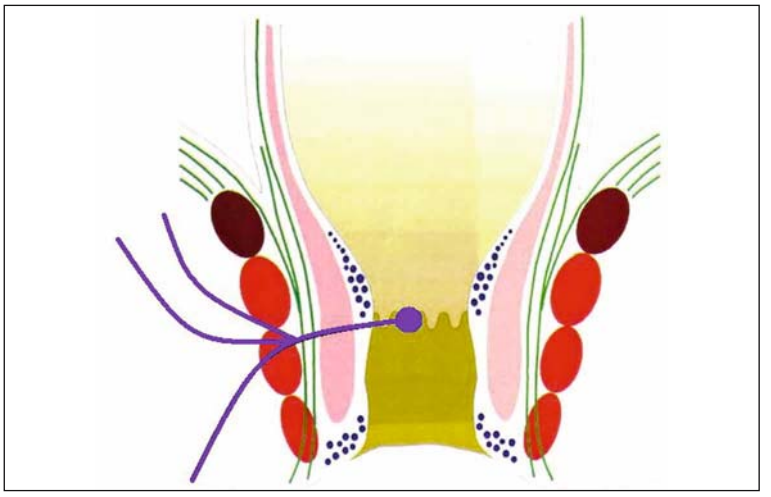

c

Fig. V.32. Posterior transsphincteric fistula (**a**) (*PT* primary tract) with two secondary transsphincteric tracts (*ST* secondary tracts) extending through the ischioanal space. Three-dimensional reconstruction (**b**). Schematic representation (**c**)

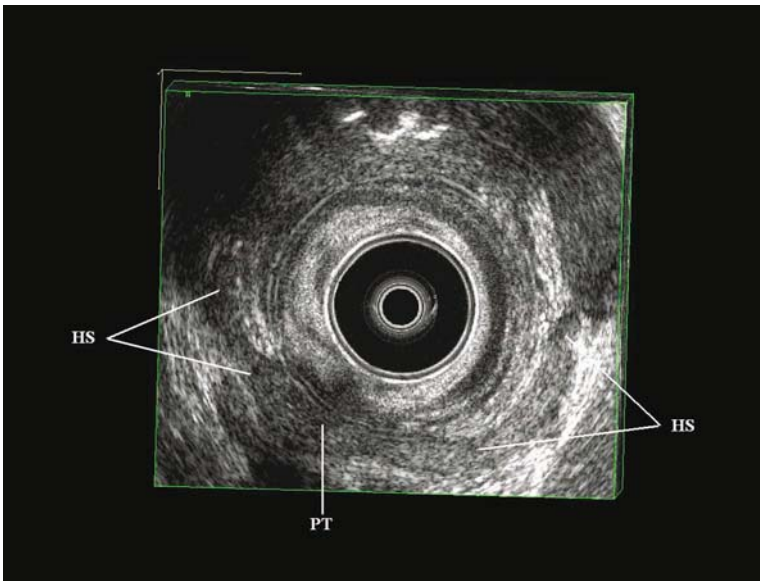

a

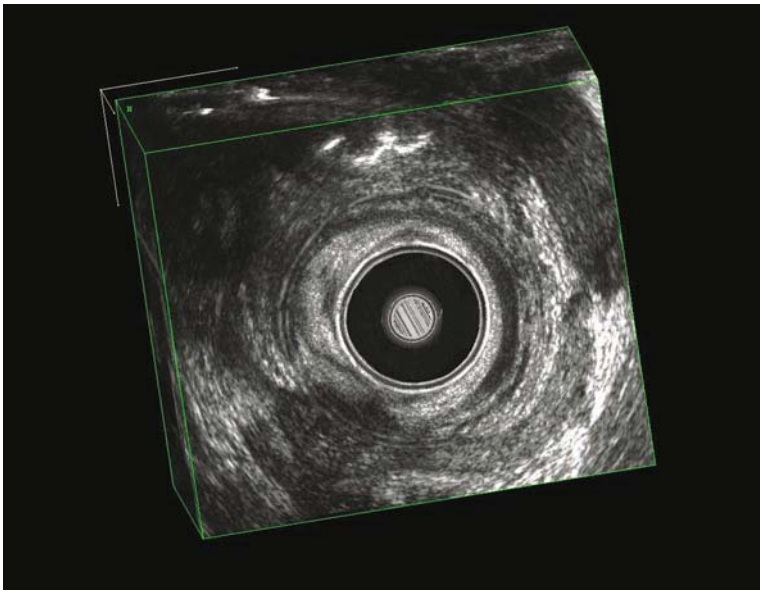

b

Fig. V.33. Posterior transsphincteric fistula (**a**) (*PT* primary tract) with horseshoe (*HS*) secondary extension through the intersphincteric space. Volume render mode (**b**)

ence between EAUS and digital examination in the assessment of internal openings. Among 35 patients with fistulas and 34 with abscesses examined by Kuntz et al. [12], EAUS showed an accuracy rate of 77.1 and 100%, respectively. Cataldo et al. [11] used EAUS intraoperatively in 24 patients in whom perianal abscesses and fistulas were suspected and correctly identified all patients with abscess, defining the relationship between the abscesses and sphincters in 63% of cases. The internal opening, however, was found in only 28% of patients. Deen et al. [6] obtained a 94% overall accuracy rate in the ultrasonographic assessment of perianal sepsis. EAUS correctly identified all primary tracts and abscesses and 91% of horseshoe tracts but could detect only 11% of the internal openings. Similar results were reported by Poen et al [7], which correctly defined primary tracts in 57% and secondary tracts in 60% of patients whereas the internal opening was identified in only 5.3% of cases. The most probable reason for the poor results in the identification of internal openings by EAUS could be the ultrasonographic criteria used. In 1998, Cho [17] pub-

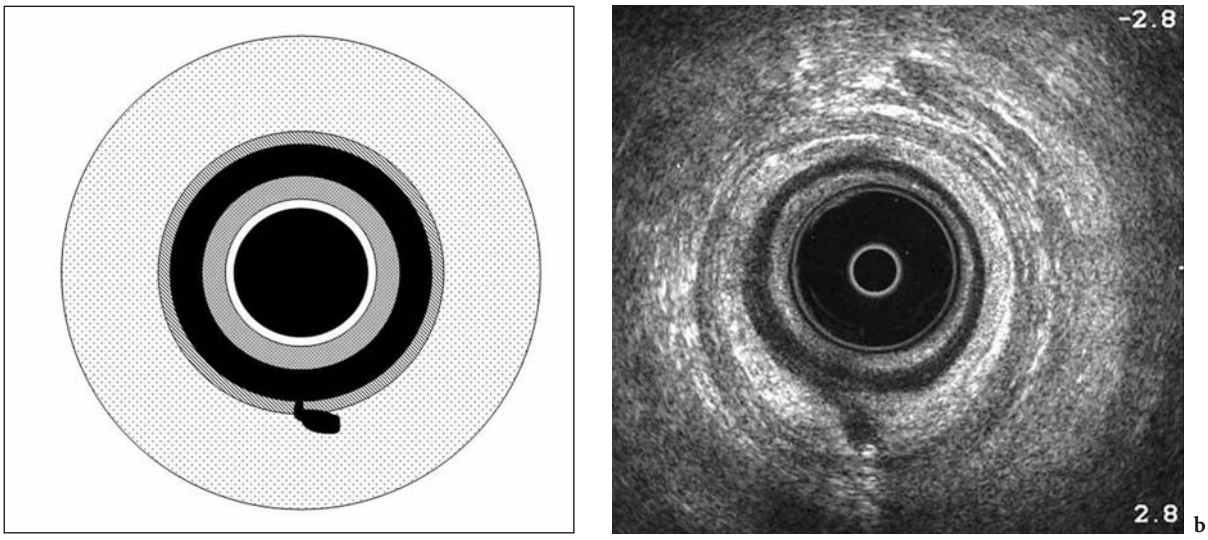

a **b**

Fig. V.34. First endosonographic criteria for the site of an internal opening according to Cho [17]: an appearance of a root-like budding formed by the intersphincteric tract, which contacts the internal sphincter (**a, b**)

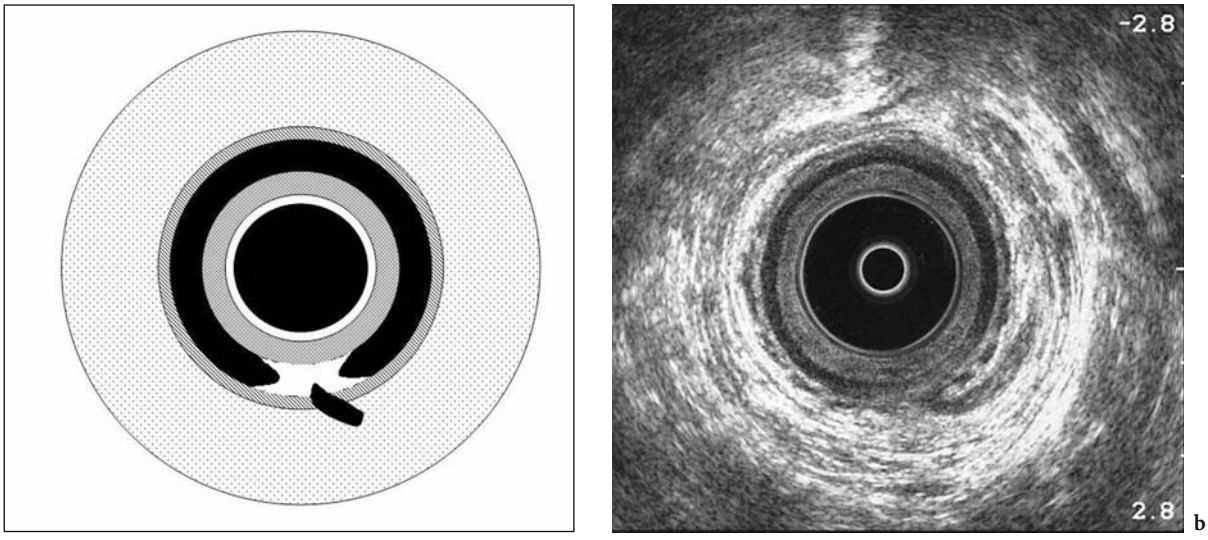

a **b**

Fig. V.35. Second endosonographic criteria for the site of an internal opening according to Cho [17]: a root-like budding with an appearance of internal sphincter defect due to inflammatory changes within the sphincter increasing its reflectivity locally (**a, b**)

lished new criteria for diagnosing internal opening. Using a combination of his three endosonographic criteria, the sensitivity of EAUS was 94%, specificity 87%, positive predictive value 81%, and negative predictive value 96%. Ratto et al. [14] showed that although EAUS improves definition of fistula anatomy compared with clinical evaluation alone, it is not accurate in defining primary tracts in approximately one half of patients. EAUS was more accurate in transsphincteric fistulas than intersphincteric tracts but could not correctly identify suprasphincteric or extrasphincteric tracts.

The major problems while investigating primary tracts with EAUS occur because of the structure alterations of the anal canal and perianal muscles and tissues, which can overstage the fistula, or poor definition of the tract when filled with inflammatory tissue, which can downstage the fistula. The disappointing results of EAUS in diagnosing extrasphincteric fistulas could be due to the echogenicity of the fistula, especially those

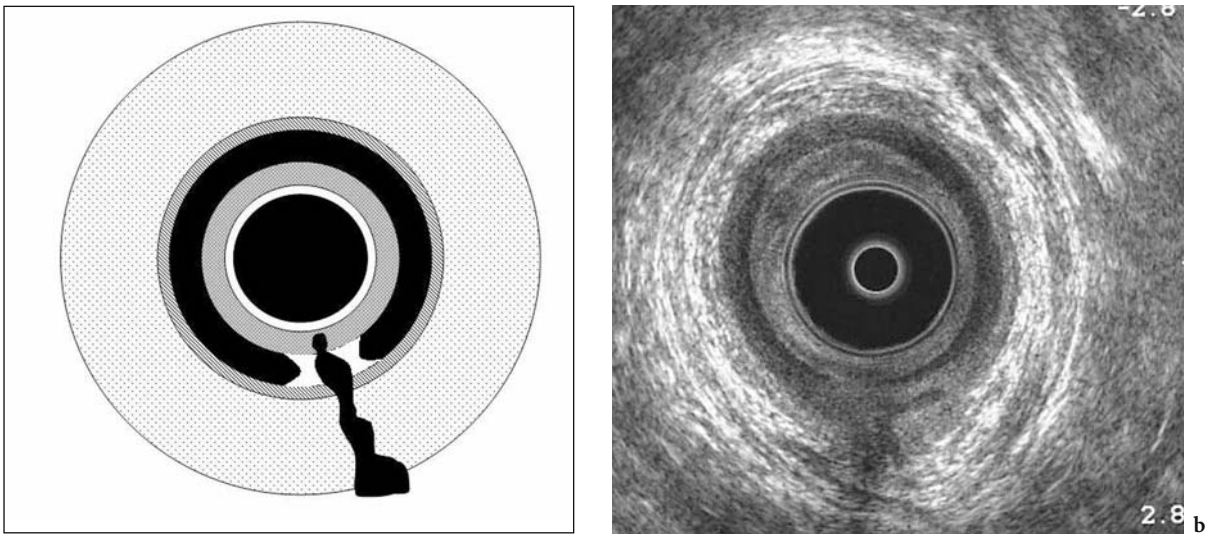

a b

Fig. V.36. Third endosonographic criteria for the site of an internal opening according to Cho [17]: a subepithelial breach connecting to the intersphincteric tract through an internal sphincter defect (**a**, **b**)

with narrow lumen, which is practically identical to the fat tissue in the ischiorectal fossa and to the short focal length of the transducer and thus prevents imaging fistula from running a large distance from the anal canal. Concerning secondary tracts, approximately two thirds of all patients were accurately identified, and false findings occurred mostly because of overstaging. EAUS did not adequately identify any secondary ischiorectal, pelvirectal, or horseshoe tracts. In comparison with clinical assessment, EAUS significantly improved accuracy in finding the internal openings, but it could not categorize it in 15–20% of patients, particularly when the opening was located in the rectum or below the dentate line.

The reported diagnostic accuracy of HPUS ranges from 71 to 95% for primary tracts and from 63 to 96.1% for secondary tracts while that of standard EAUS ranges from 50 to 91.7% for the primary tract and from 60 to 68% for secondary tracts (Table V.1). The highest concordance is usually reported for primary transsphincteric fistulas while the major of diagnostic difficulty is still the adequate identification of primary supra- and extrasphincteric fistulas. HPUS also can contribute to a more accurate identification of the internal opening. In comparison to results reported using standard EAUS with an accuracy ranging from 5.3 to 93.5%, the reported accuracy of HPUS is higher, ranging from 48 to 96.6%. Cheong et al. [26] were the first to describe the use of HPUS in order to accentuate tissue interface layers at the level of the fistula tract and suggested its usefulness particularly in recurrent and complex fistulas. Subsequently, in a prospective study of 21 patients with fistula-in-ano, Poen et al. [7] reported an HPUS accuracy rate of 95% for primary tracts, 71% for secondary extensions, and 48% for internal openings. Ratto et al. [14] correctly identified 75% of primary tracts using HPUS, and compared with EAUS, this method was more accurate in identifying transsphincteric and intersphincteric tracts. However, both EAUS and HPUS were unable to identify suprasphincteric and extrasphincteric tracts. Approximately 85% of secondary tracts were correctly staged with HPUS, with an accuracy of nearly 90% for intersphincteric and ischiorectal tracts. HPUS failed, however, to improve the ability of EAUS to identify the internal openings, particularly when located below the dentate line or in the rectal ampulla. In this regard, Moscowitz et al. [27] reported a 61.1% correlation between HPUS and surgical findings of the internal opening, with a positive predictive value of 84%. Poor results were reported by Ortiz et al. [28], who correctly identified an internal opening endosonographically in 62.5% of patients (32% with intersphincteric fistulas, 77% with transsphincteric fistulas, and 17% with suprasphincteric fistulas).

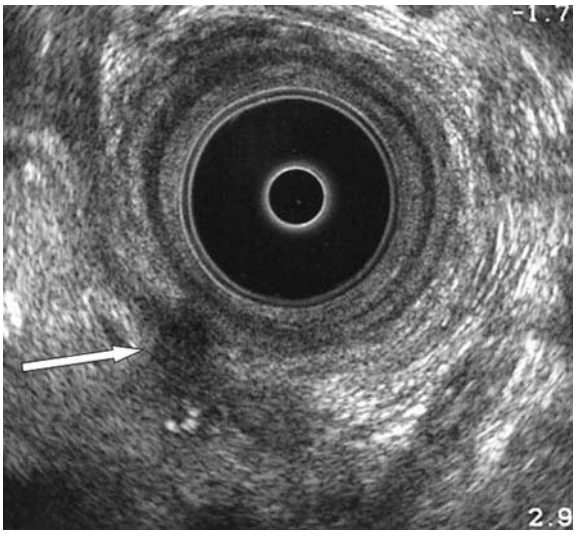

a

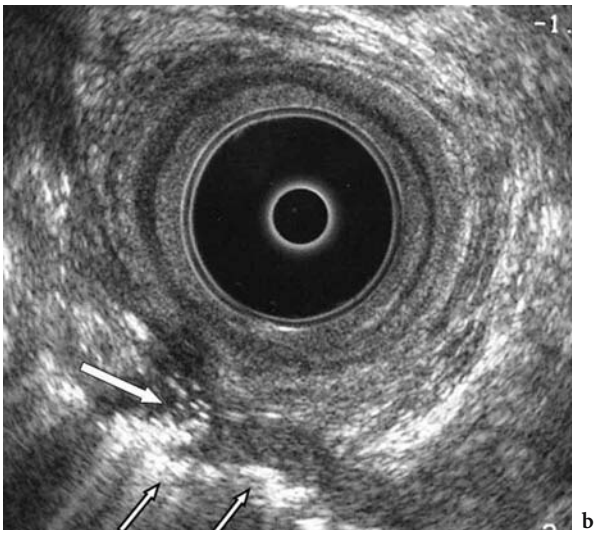

b

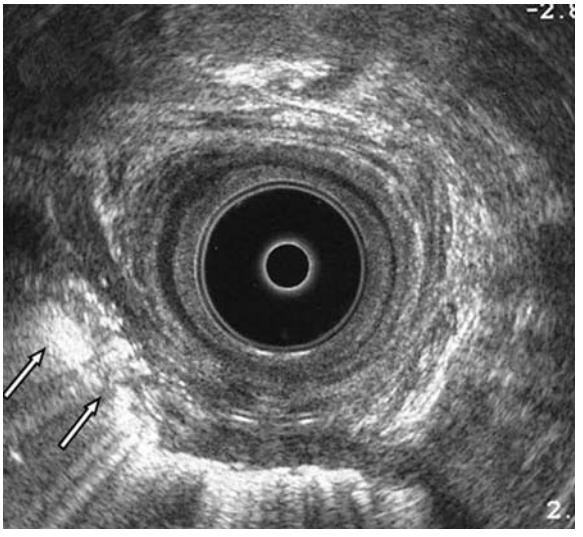

c

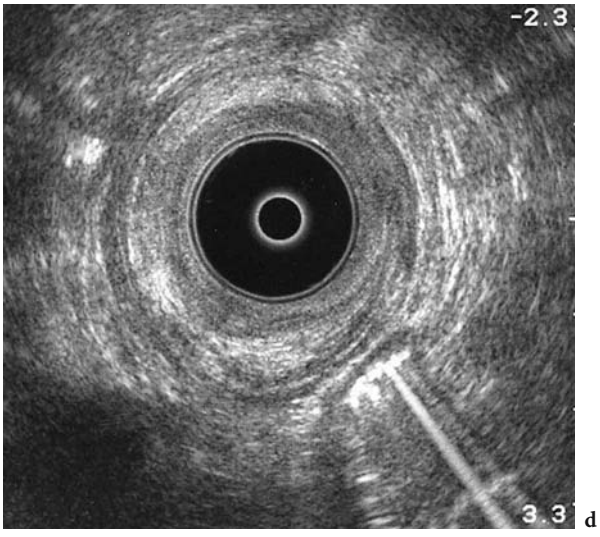

d

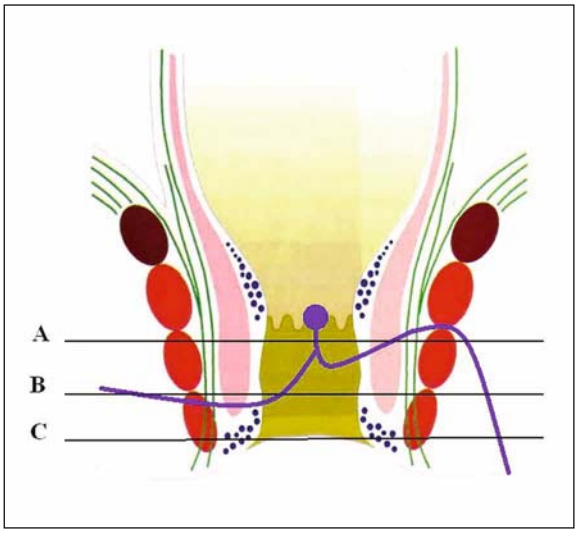

e

Fig. V.37. Posterior transsphincteric tract extending through the external sphincter (*arrow*). No secondary extensions are clearly visible. Higher part of the anal canal (level A) (**a**). After hydrogen peroxide, fistula tract becomes hyperechoic (*large arrow*), and a secondary hyperchoic horseshoe extension through the left and right ischioanal spaces (*small arrows*) becomes evident. Middle part of the anal canal (level B) (**b**, **c**). Lower part of the anal canal (level C) subcutaneous echogenic area at 5 o'clock (external opening) (**d**). Schematic representation of the fistulous tract at the three different levels (**e**)

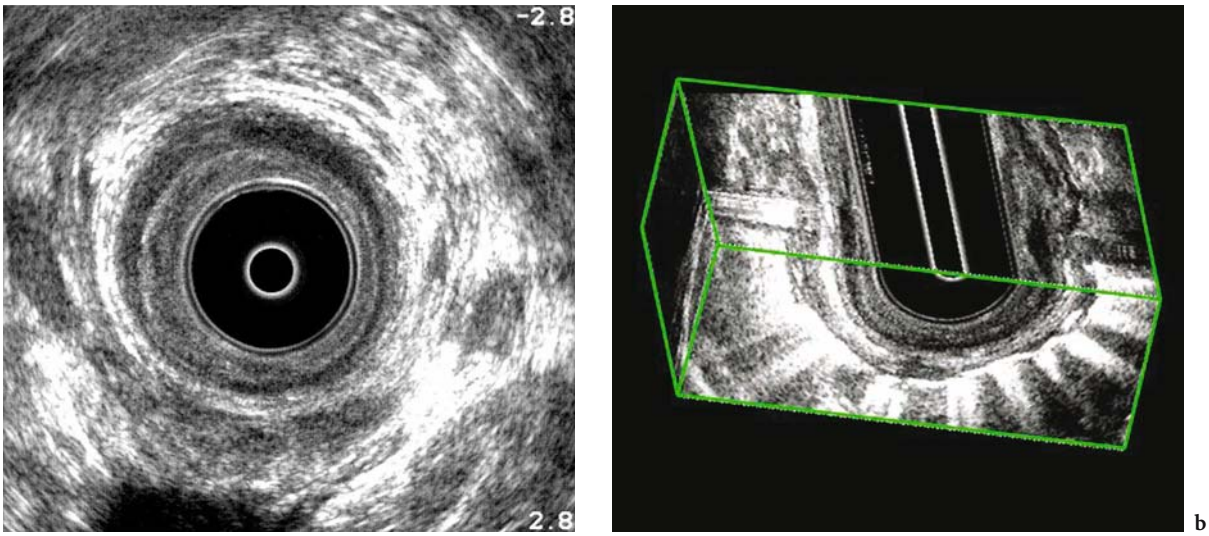

a b

Fig. V.38. Horseshoe intersphincteric fistula (**a**). After hydrogen peroxide injection, the bubbles produce a very strong reflection at the gas/tissue interface, which blanks out any detail deep beyond this interface (**b**). All information deep beyond the inner surface of the tract is lost

There were no statistically significant differences in the identification of an internal opening by EAUS between recurrent fistula (67%) and non-recurrent fistula (62%). They concluded that the accuracy of HPUS for the identification of internal openings is still insufficient to justify preoperative endosonography as a diagnostic method for routine use in patients with fistula-in-ano. Navarro et al. [19] reported excellent results with hydrogen peroxide enhancement. HPUS was able to identify the internal opening in 94% of cases and whether the tract was linear or curvilinear in 95% of cases. The ultrasound level coincided with surgical findings in 85% of patients, and chronic fistula cavities were confirmed by surgery in 75% of patients. These results were confirmed by

Table V.1. Comparison of endoanal ultrasonography (EAUS) and hydrogen-peroxide-enhanced transanal ultrasound (HPUS) in the evaluation of fistula-in-ano. Review of the literature

Authors	Patients (no.)	EAUS probe	Primary tract		Secondary tract		Internal opening	
			EAUS	HPUS	EAUS	HPUS	EAUS	HPUS
Law et al. [10]	22	7 MHz	95%		100%		82%	
Seow-Choen et al. [5]	36	7 MHz	75%				75%	
Lunniss et al. [20]	20	7 MHz	70%				70%	
Cataldo et al. [11]	24	7 MHz	63%				28%	
Deen et al. [6]	18	7 MHz	100%		91%		11%	
Hussain et al. [21]	28	7 MHz	36%				57%	
Kuntz et al. [12]	35	7 MHz	77%					
Poen et al. [7]	21	7 MHz	62%	95%	60%	71%	14%	48%
Ratto et al. [14]	26	10 MHz	50%	77%	65%	88%	54%	54%
Gustafsson et al. [22]	23	10 MHz	61%		65%		74%	
Navarro et al. [23]	55	10 MHz	85%				96%	
Joo et al. [24]	25	10 MHz	76%				64%	
Ratto et al. [25]	89	10 MHz	84.3%	97.8%	80.9%	98.8%	87.6%	96.6%

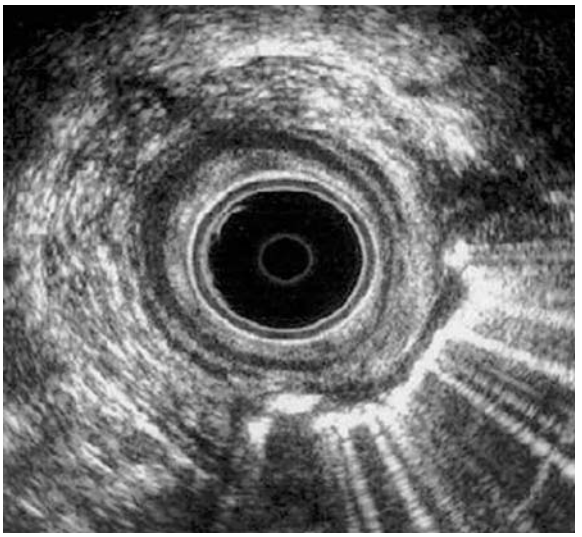

a

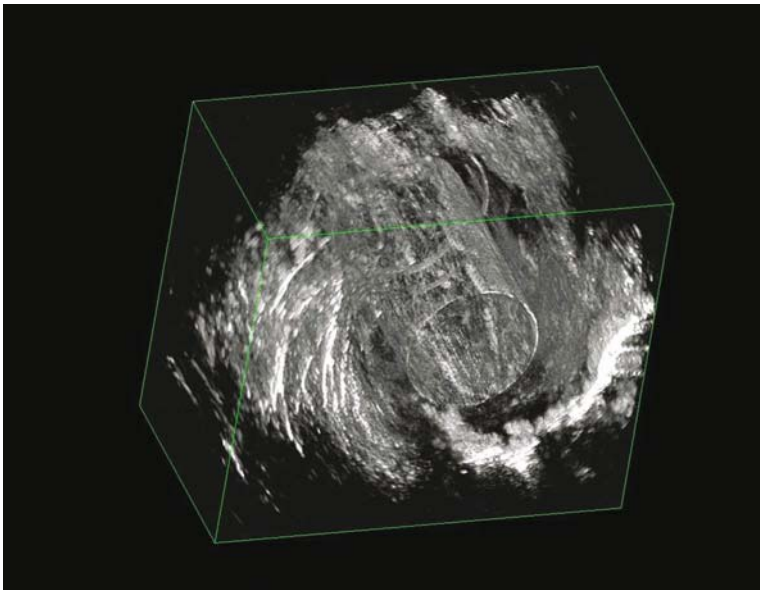

b

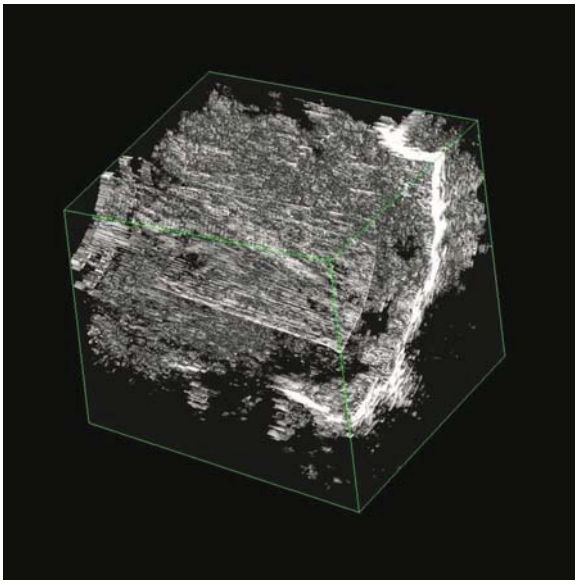

c

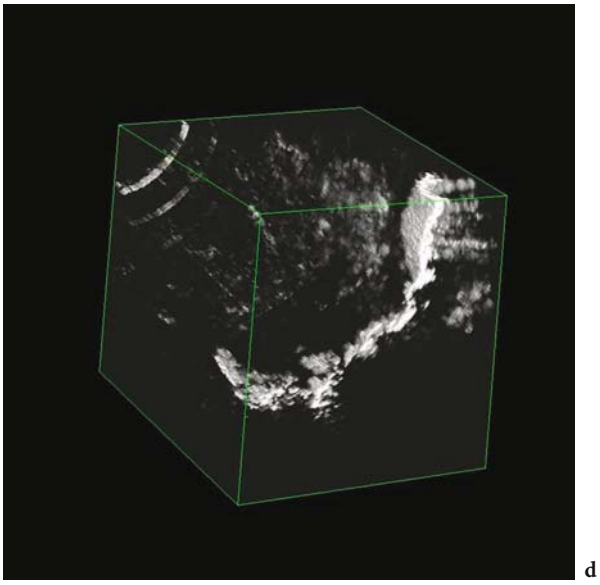

d

Fig. V.39. After hydrogen peroxide injection into a transsphincteric tract, reflections from gas bubbles produce an acoustic shadowing deep beyond the tract (**a**). To reduce this potential pitfall of imaging, a volume-rendered three-dimensional data set can facilitate the following of a tortuous fistula tract due to the transparency and depth information (**b–e**)

Sudol-Szopinska et al. [15], who found HPUS significantly increased the accuracy of standard noncontrast EAUS in identifying internal opening (89% vs. 65%, respectively) and in differentiating simple from complex tracts (92% vs.75%, respectively; $p<0.00001$).

More recently, the availability of the 3-D imaging system has provided another very useful tool for accurate assessment of endoanal and endorectal ultrasound examination. With regard to anal fistulas, with this method, the operator can review the entire series of ultrasound images reconstructed along all planes desired (coronal, sagittal, transverse, oblique). Buchanan et al. [29], in 19 patients with recurrent or complex fistulas, reported accurate results in detecting primary tracts (81%), secondary tracts (68%), and internal openings (90%). The addition of hydrogen peroxide (3-D HPUS) did not improve these features (accuracies of 71%, 63%, and 86%, respectively). West et al. [30] reported that 3-D HPUS and endoanal MRI are equally adequate for the evaluation of perianal fistulas. The methods agreed in 88% of cases for the primary fistula tract, in 90% for the location of the internal opening, in 78% for secondary tracts, and in 88% for fluid collections. Using 3-D imaging, Ratto et al. [25] reported an accuracy of 98.5% for primary tracts, 98.5% for secondary tracts, and 96.4% for internal openings compared with 89.4%, 83.3%, and 87.9%, respectively, when the two-dimensional (2-D) system was used. Our experience [31] with 57 patients with perianal fistulas confirms that 3-D reconstructions improves the accuracy of EAUS in the identification of the internal opening compared with standard ultrasonography (2-D EAUS: 66.7% vs. 3-D EAUS: 89.5%; $P=0.0033$). Primary tracts, secondary tracts, and abscesses were correctly evaluated by both procedures.

References

1. Joy HA, Williams JG (2002) The outcome of surgery for complex anal fistula. Colorectal Dis 4:254–261
2. Corman ML (1993) Anorectal abscess and fistula. In: Corman ML (ed) Colon and rectal surgery, 3rd edn. Lippincott, Philadelphia, pp 133–187
3. Parks AG, Gordon PH, Hardcastle JD (1976) A classification of fistula-in-ano. Br J Surg 63:1–12
4. Kuijpers HC, Schulpen T (1985) Fistulography for fistula-in-ano: is it useful? Dis Colon Rectum 28:103–104
5. Seow-Choen F, Burnett S, Bartram CI, Nicholls RJ (1991) Comparison between anal endosonography and digital examination in the evaluation of anal fistulae. Br J Surg 78:445–447
6. Deen KI, Williams JG, Hutchinson R (1994) Fistulas in ano: endoanal ultrasonographic assessment assists decision making for surgery. Gut 35:391–394
7. Poen AC, Felt-Bersma RJF, Eijsbouts QA et al (1998) Hydrogen peroxide-enhanced transanal ultrasound in the assessment of fistula-in-ano. Dis Colon Rectum 41:1147–1152
8. Weisman RI, Orsay CP, Pearl RK, Abcarian H (1991) The role of fistulography in fistula-in-ano. Report of five cases. Dis Colon Rectum 34:181–184
9. Shouler PJ, Grimley RP, Keighley MR, Alexander-Wiliams J (1986) Fistula-in-ano is usually simple to manage surgically. Int J Colorectal Dis 1:113–115
10. Law PJ, Talbot RW, Bartram CI, Northover JMA (1989) Anal endosonography in the evaluation of perianal sepsis and fistula in ano. Br J Surg 76:752–755
11. Cataldo PA, Senagore A, Luchtefeld MA (1993) Intrarectal ultrasound in the evaluation of perirectal abscesses. Dis Colon Rectum 36:554–558
12. Kuntz C, Glaser F, Buhr HJ, Herfarth C (1994) Endoanal ultrasound. Indications and results. Chirurg 65:352–357
13. Lindsey I, Humphreys MM, George BD, Mortensen NJ (2002) The role of anal ultrasound in the management of anal fistulas. Colorectal Dis 4:118–122
14. Ratto C, Gentile E, Merico M et al (2000) How can the assessment of fistula-in-ano be improved? Dis Colon Rectum 43:1375–1382
15. Sudol-Szopinska I, Szczepkowski M, Panorska AK et al (2004) Comparison of contrast-enhanced with non-contrast endosonography in the diagnostics of anal fistulas. Eur Radiol 14:2236–2241
16. Sloots CEJ, Felt-Bersma RJF, Poen AC et al (2001) Assessement and classification of fistula-in-ano in patients with Crohn's disease by hydrogen peroxide enhanced transanal ultrasound. Int J Colorectal Dis 16:292–297
17. Cho DY (1999) Endosonographic criteria for an internal opening of fistula-in-ano. Dis Colon Rectum 42:515–518
18. Kruskal JB, Kane RA, Morrin MM (2001) Peroxide-enhanced anal endosonography: technique, image interpretation and clinical applications. Radiographics 21:S173–S189
19. Navarro-Luna A, Garcia-Domingo MI, Rius-Macias J,

Marco-Molina C (2004) Ultrasound study of anal fistulas with hydrogen peroxide enhancement. Dis Colon Rectum 47:108–114

20. Lunniss PJ, Kamm MA, Phillips RKS (1994) Factors affecting continence after surgery for anal fistula. Br J Surg 81:1382–1385
21. Hussain SM, Stoker J, Schouten WR et al (1996) Fistula-in-ano: endoanal sonography versus endoanal MR imaging in classification. Radiology 200:475–481
22. Gustafsson UM, Kahvecioglu B, Astrom G et al (2001) Endoanal ultrasound or magnetic resonance imaging for preoperative assessment of anal fistula: a comparative study. Colorectal Dis 3:189–197
23. Navarro A, Rius J, Collera P et al (1998) Anal fistulas: results of ultrasonographic studies. Dis Colon Rectum 41:A57
24. Joo JS, Son KS, Lee HS, Lee SK (1998) Preoperative evaluation of anal fistula by endorectal ultrasonography. Dis Colon Rectum 41:A46–47
25. Ratto C, Grillo E, Parello A et al (2005) Endoanal ultrasound-guided surgery for anal fistula. Endoscopy 37:1–7
26. Cheong DM, Nogueras JJ, Wexner SD, Jagelman DG (1993) Anal endonography for recurrent anal fistulas: image enhancement with hydrogen peroxide. Dis Colon Rectum 36:1158–1160
27. Moscowitz I, Baig MK, Noguearas JJ et al (2003) Accuracy of hydrogen peroxide enhanced endoanal ultrasonography in assessment of the internal opening of an anal fistula complex. Tech Coloproctol 7:133–137
28. Ortiz H, Marzo J, Jemenez G, DeMiguel M (2001) Accuracy of hydrogen peroxide-enhanced ultrasound in the identification of internal openings of anal fistulas. Colorectal Dis 4:280–283
29. Buchanan GN, Halligan S, Bartram CI et al (2004) Clinical examination, endosonography and MR imaging in preoperative assessment of fistula in ano: comparison with outcome-based reference standard. Radiology 233:674–681
30. West RL, Dwarkasing S, Felt-Bersma RJF et al (2004) Hydrogen peroxide-enhanced three-dimensional endoanal ultrasonography and endoanal magnetic resonance imaging in evaluating perianal fistulas: agreement and patient preference. Eur J Gastroenterol Hepat 16:1319–1324
31. Santoro GA, Ratto C, Di Falco G (2004) Three-dimensional reconstructions improve the accuracy of endoanal ultrasonography in the identification of internal openings of anal fistulas. Colorectal Dis 6 [Suppl 2]:P214

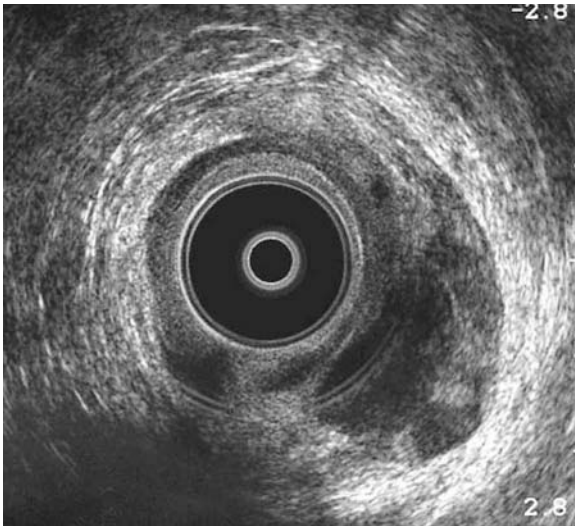

a

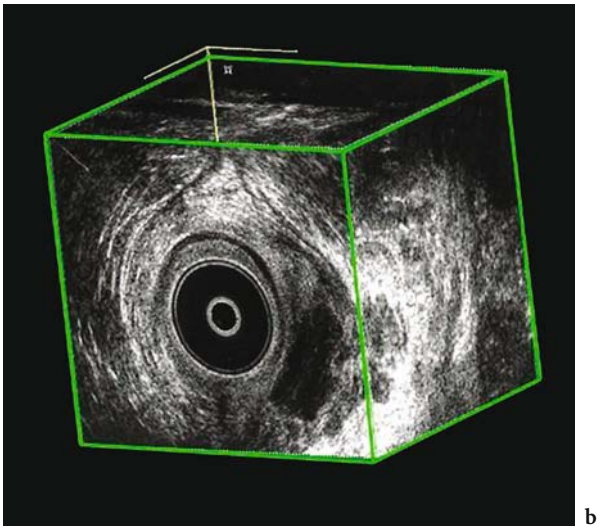

b

Case V.1. A 23-year-old man complaining of perianal pain. Physical examination reveals a left lateral, superficial, tender mass outside the anal verge. Axial endosonographic image of lower anal canal level reveals a large hypoechoic area (**a**). Three-dimensional endoanal ultrasonography confirms the presence of an acute superficial abscess (**b**). The patient underwent immediate incision and drainage

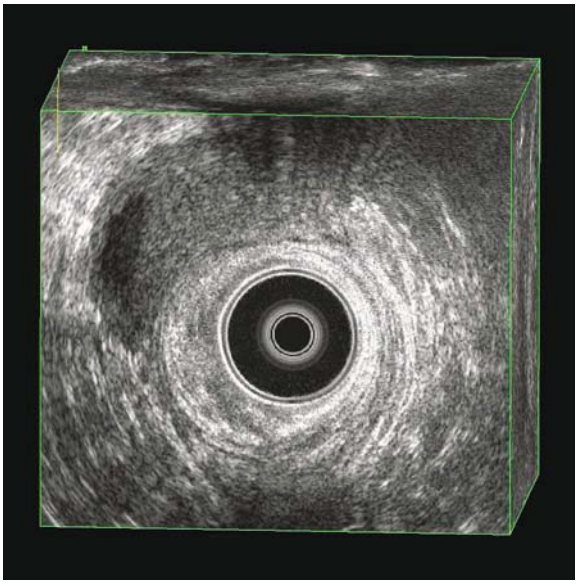

a

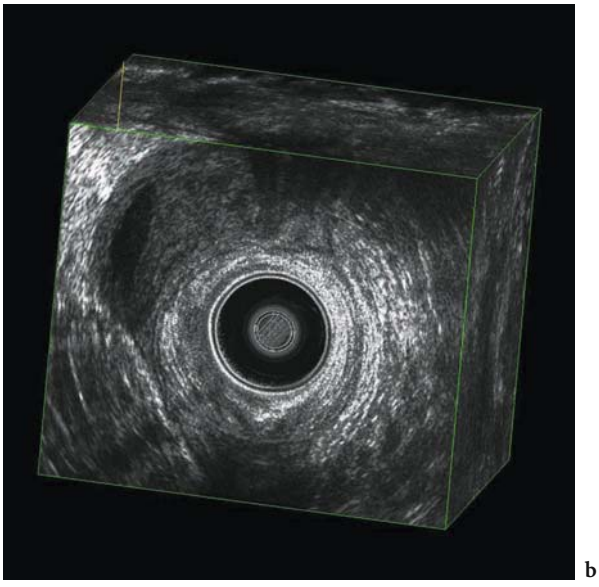

b

Case V.2. A 47-year-old man complaining of fever and perianal pain. Physical examination reveals an anterior, superficial, tender mass outside the anal verge. Three-dimensional reconstruction in the axial plane reveals a large hypoechoic area (**a**). Volume render mode confirms the presence of an acute superficial abscess (**b**). The patient underwent immediate incision and drainage

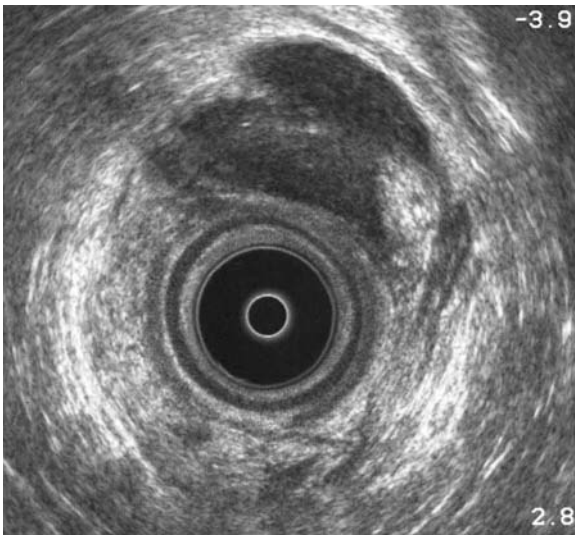

a

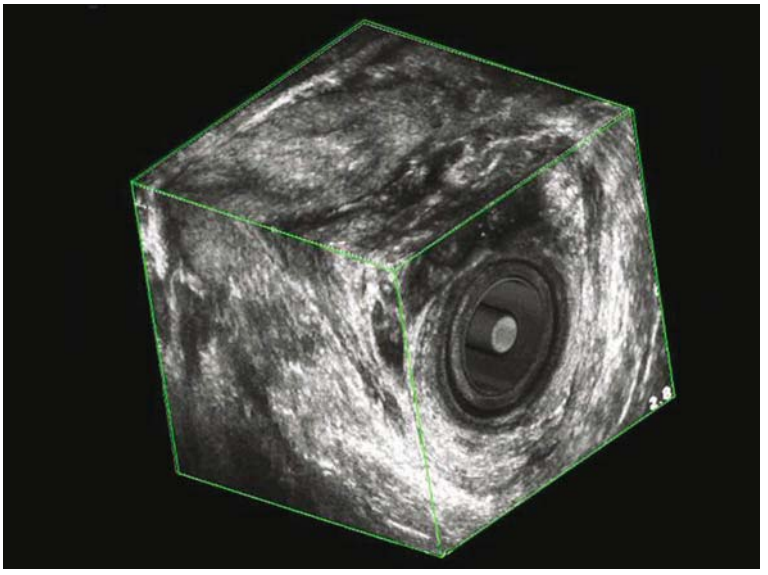

b

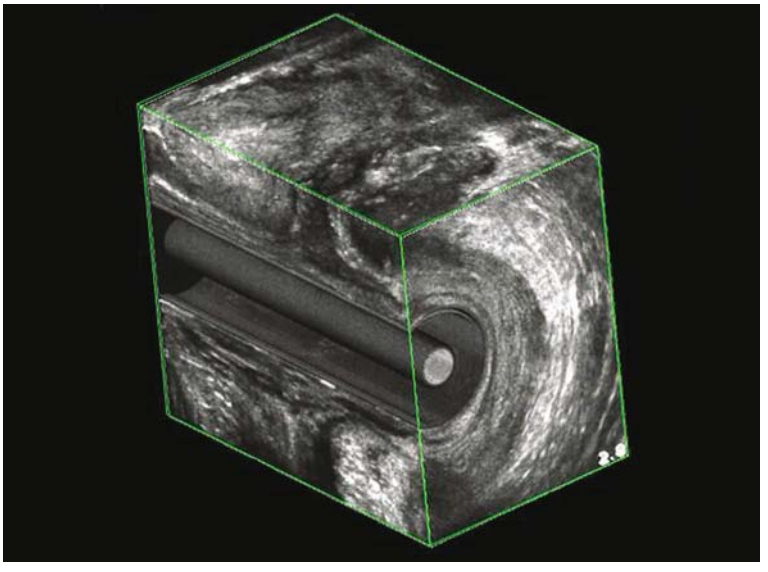

c

Case V.3. A 63-year-old man complaining of fever and perirectal pain. Digital rectal examination reveals an anterior, tender mass at the dentate line level 2 cm from the anal verge. Axial endosonographic image of mid anal canal level reveals a large hypoechoic area in the anterior intersphincteric zone (**a**). Three-dimensional endoanal ultrasonography scans with volume render mode confirm the presence of an acute anterior intersphincteric abscess (**b**, **c**). The patient underwent immediate drainage through the intersphincteric space

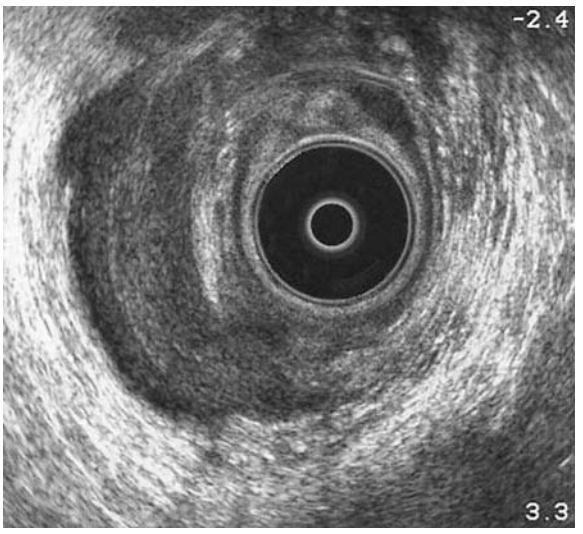

a

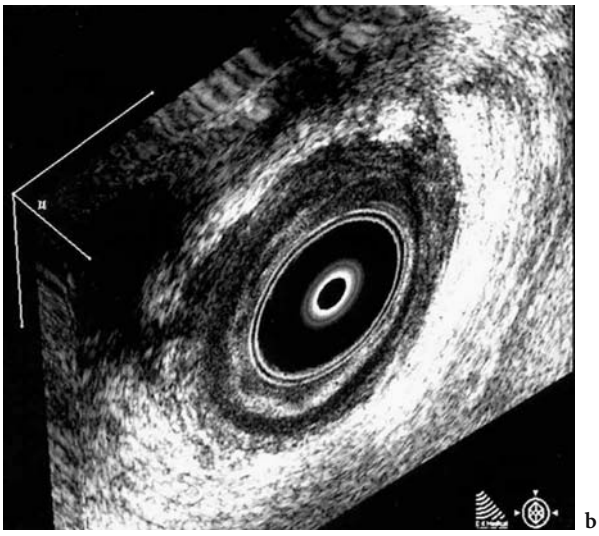

b

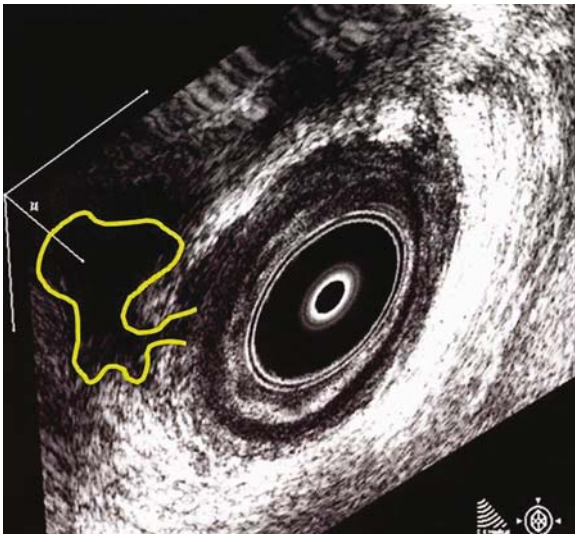

c

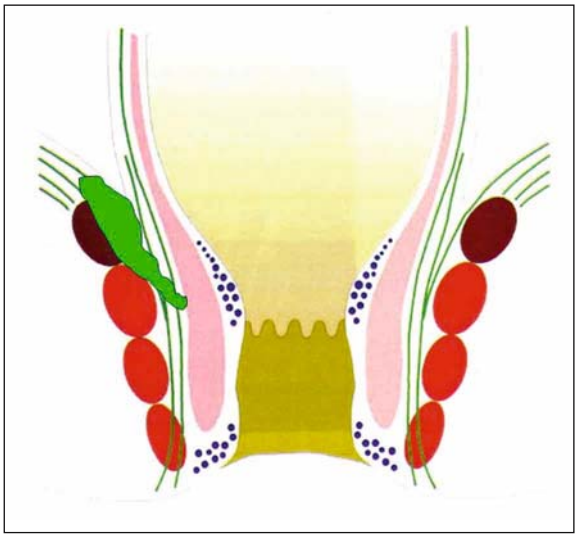

d

Case V.4. A 45-year-old woman complaining of fever and perirectal pain. Digital rectal examination reveals a right lateral, supralevator, tender mass at 4 cm from the anal verge. Axial endosonographic image of the upper anal canal level reveals a large hypoechoic dishomogeneous area in the right lateral supralevator space (**a**). Three-dimensional endoanal ultrasonography reconstruction confirms the presence of an acute supralevator abscess (**b, c**). Drawing in the coronal plane (**d**)

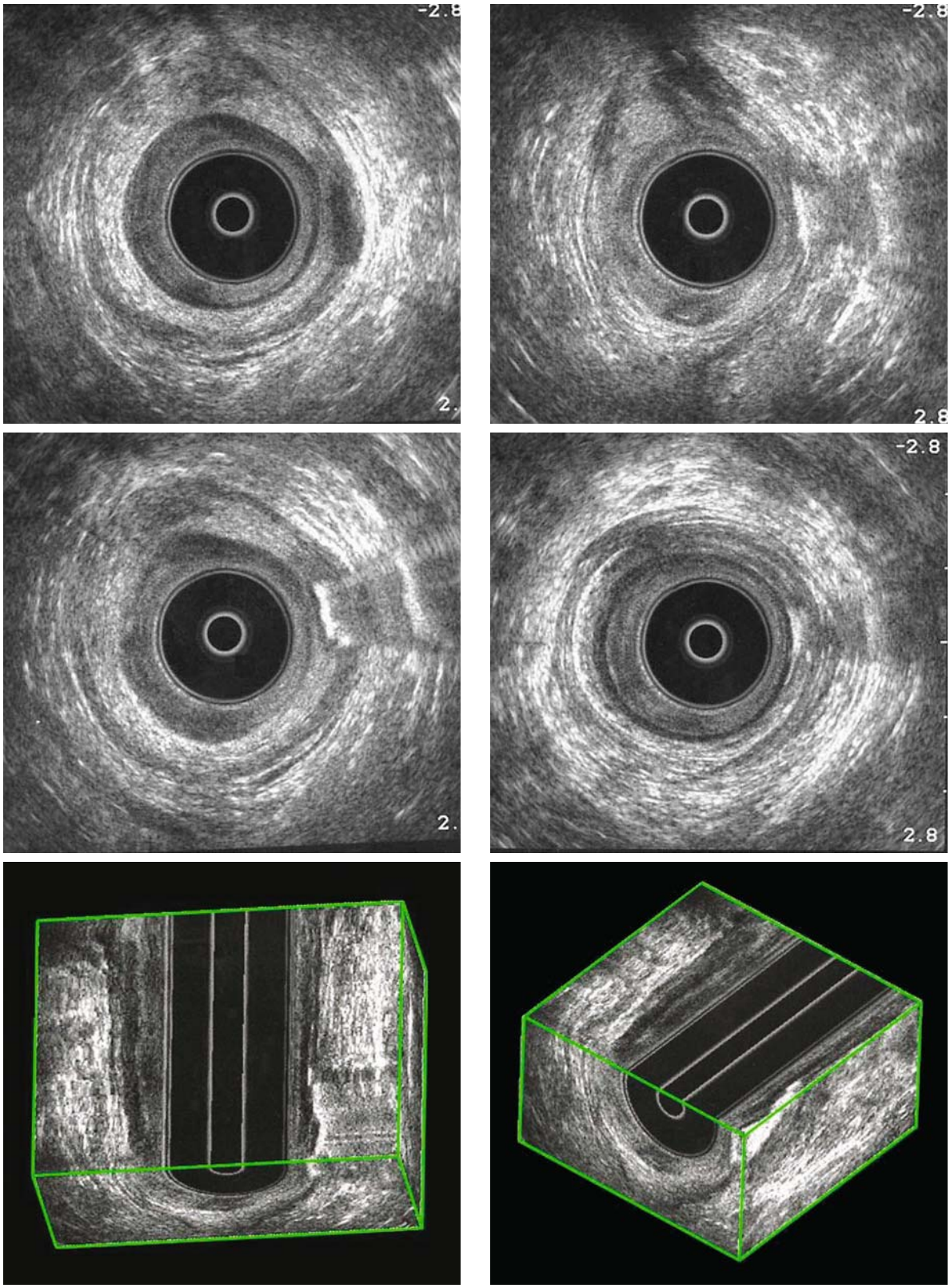

Case V.5. A 57-year-old man complaining of perianal purulent discharge from an external orifice at the 3 o'clock position (left lateral side) immediately adjacent to the anal canal. Axial endosonographic image of mid anal canal level reveals a hypoechoic area in the intersphincteric zone at the 3 o'clock position (**a**). After administration of peroxide, endoanal ultrasonography scans show a direct communication that extends from the skin (**b**) through the lower anal canal (**c**) to the mid anal canal (**d**), demonstrating a simple intersphincteric fistula. Three-dimensional hydrogen-peroxide-enhanced ultrasonography confirms the presence of left lateral intersphincteric fistula (**e**, **f**)

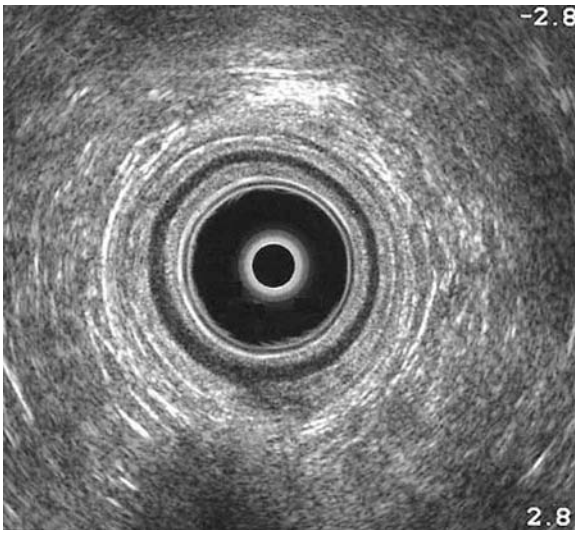

a

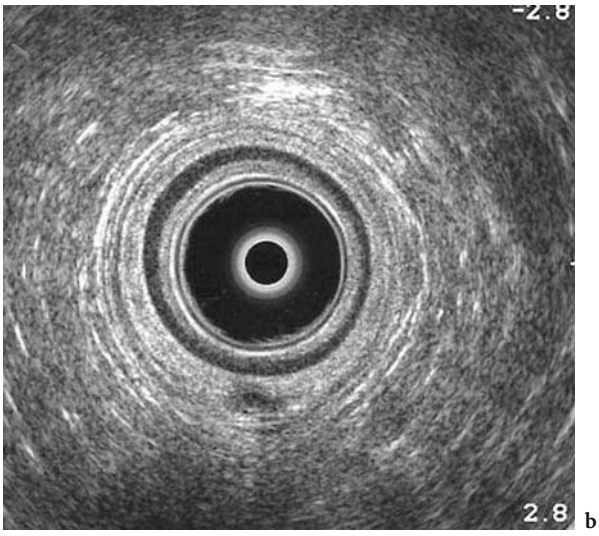

b

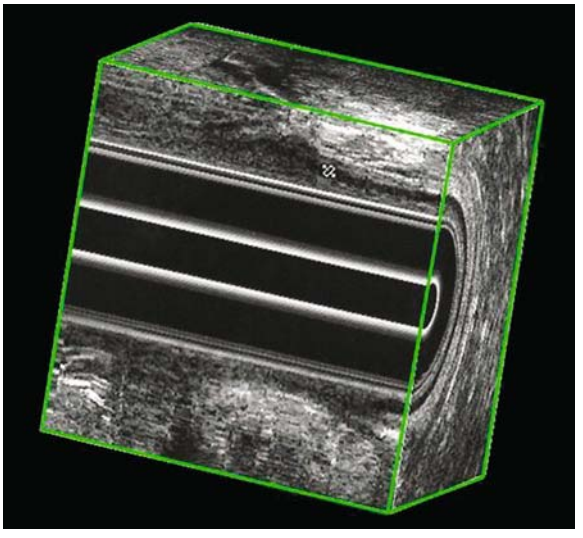

c

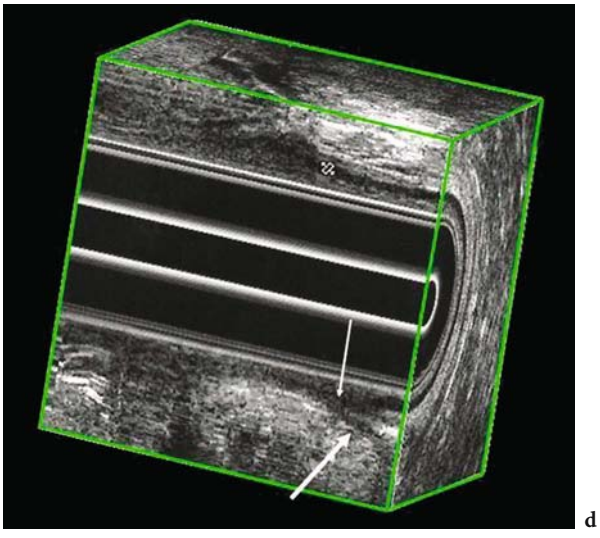

d

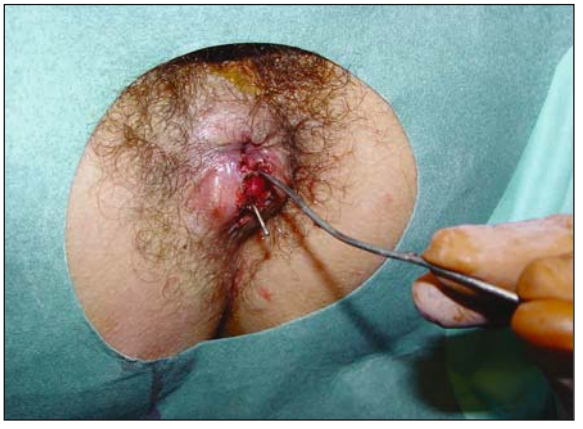

e

Case V.6. A 28-year-old woman complaining of purulent discharge from the anus. Axial endosonographic images of mid anal canal level reveal a hypoechoic area in the posterior intersphincteric zone (**a, b**). Three-dimensional reconstruction in the sagittal plane confirms an intersphincteric fistula, appearing as a band of poor reflectivity within the intersphincteric plane (*large arrow*), communicating with the anal canal (internal orifice; *small arrow*) (**c, d**). The patient underwent an unroofing procedure (**e**)

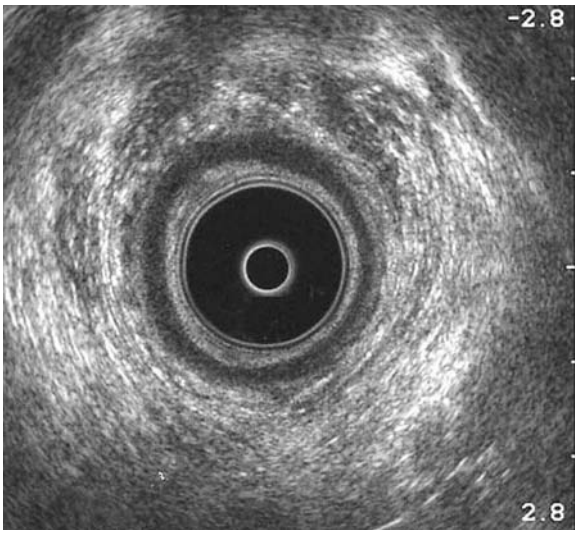

a

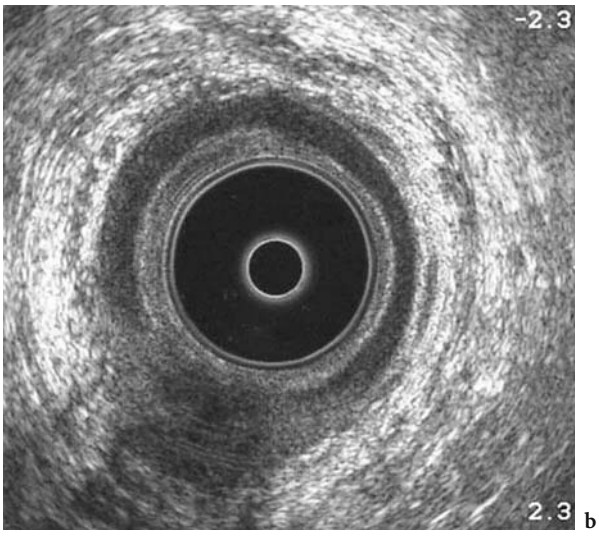

b

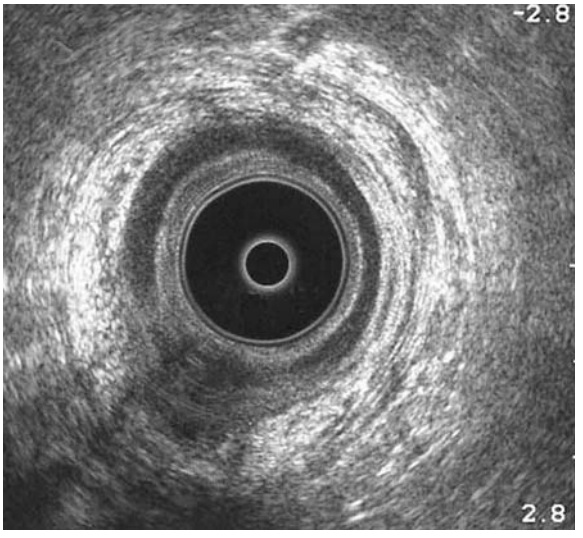

c

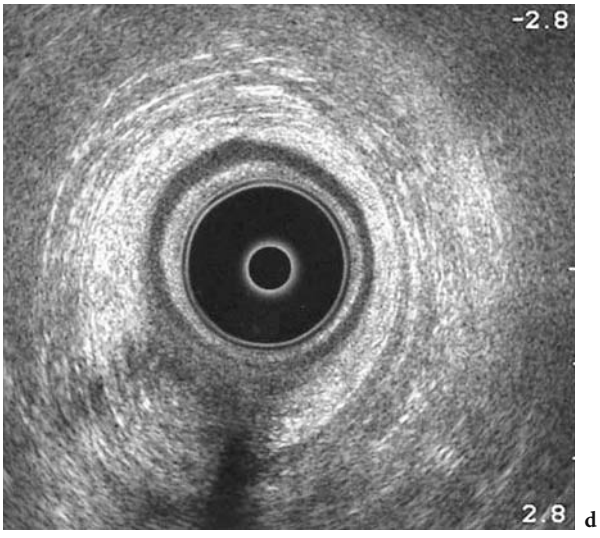

d

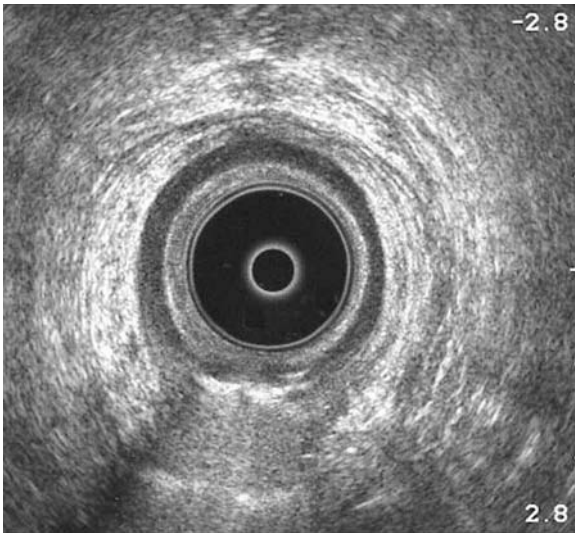

e

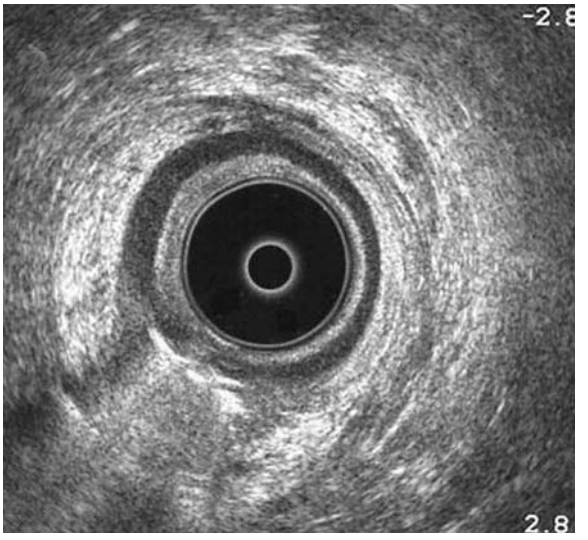

f

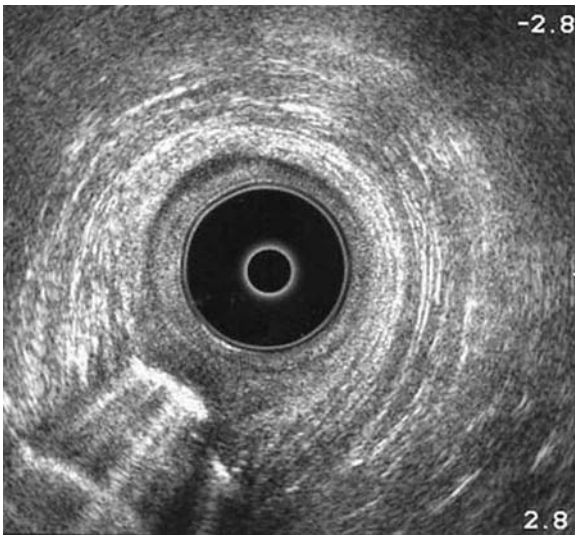

g

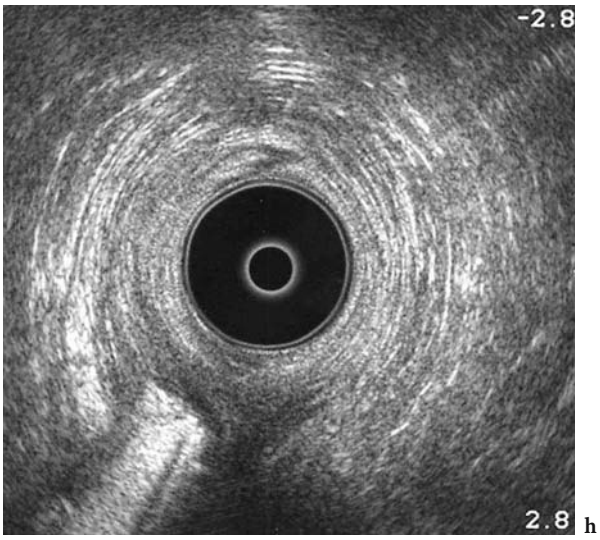

h

Case V.7. A 53-year-old man complaining of recurrent perianal purulent discharge. Physical examination reveals a cutaneous opening at the 6 o'clock position. Axial endosonographic image at the upper anal canal level shows a normal anatomy (**a**). At mid anal canal level, endoanal ultrasonography (EAUS) scans reveal a posterior hypoechoic tract extending through the external sphincter, with an appearance of internal sphincter defect at the 6 o'clock position (**b**, **c**) (second endosonographic criteria for the site of an internal opening according to Cho [17]). The fistula also tracks downward at the lower anal canal level (**d**). After peroxide injection, the EAUS scans confirm immediate communication with the anal canal (**e**, **f**) with the transsphincteric fistula extending caudally (**g**, **h**)

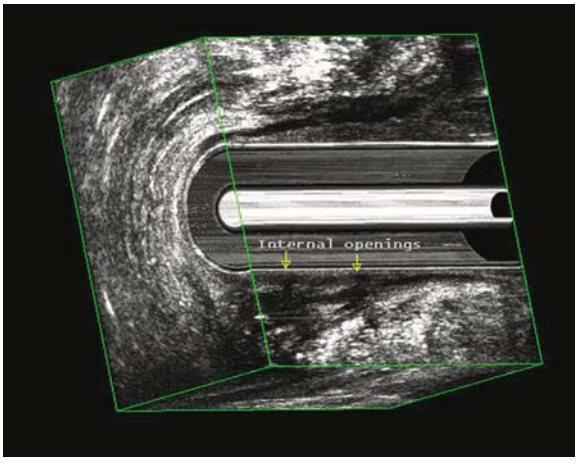

a

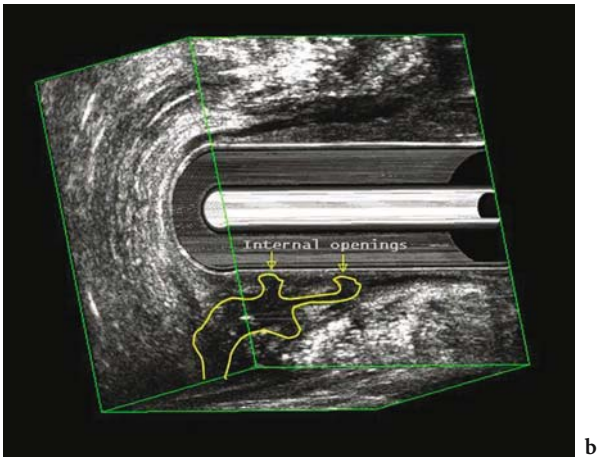

b

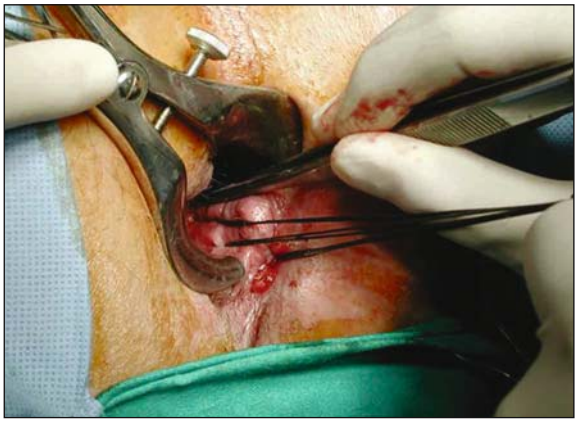

c

Case V.8. A 43-year-old woman complaining of anal pain and perianal purulent discharge from an external orifice at the 6 o'clock position. Sagittal view from a three-dimensional data set shows a transsphincteric tract with two internal openings that traverses the middle part of the external sphincter (**a**, **b**). At surgery, the presence of two internal openings was confirmed, and two cutting setons were inserted through this complex fistulous tract (**c**)

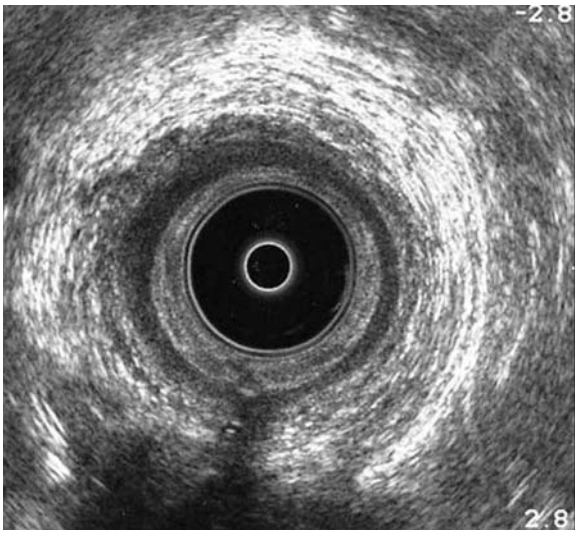

a

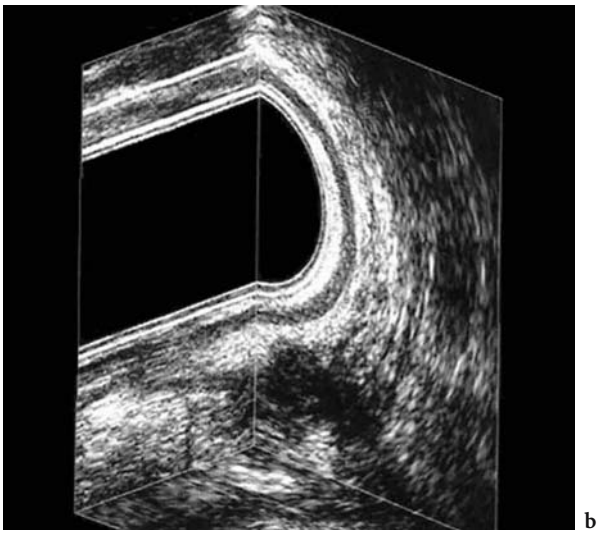

b

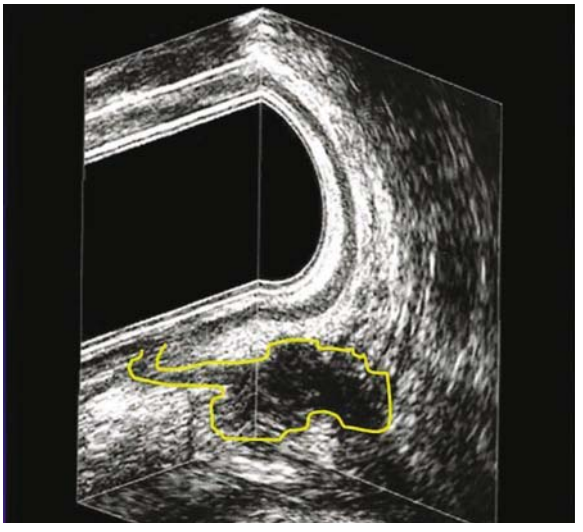

c

Case V.9. A 53-year-old man complaining of recurrent perianal purulent discharge. Physical examination reveals a cutaneous opening at the 6 o'clock position. Axial endosonographic image at mid anal canal level shows a posterior hypoechoic tract extending through the internal and external sphincters at the 6 o'clock position (**a**) (third endosonographic criteria for the site of an internal opening according to Cho [17]). Three-dimensional ultrasonography scan confirms the presence of a transsphincteric fistula at the 6 o'clock position, traversing the middle part of the external sphincter and communicating with a small perianal abscess (**b**, **c**)

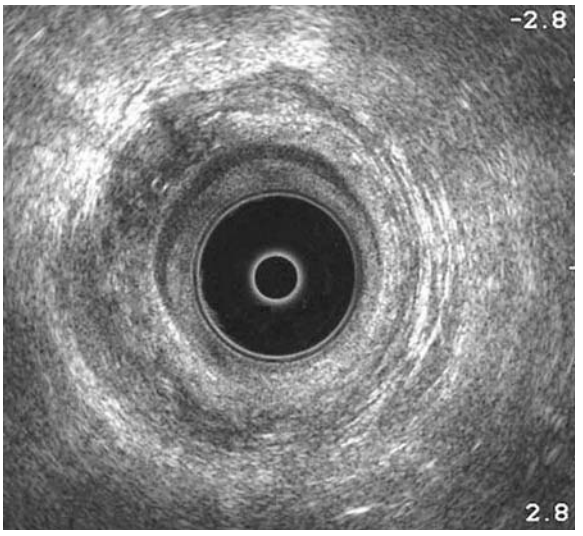

a

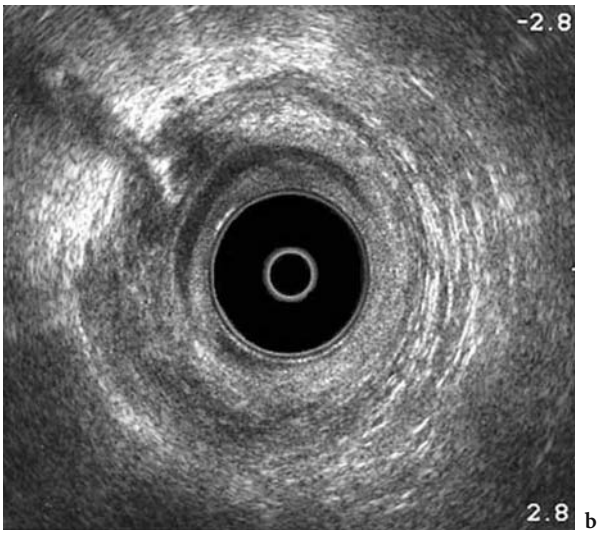

b

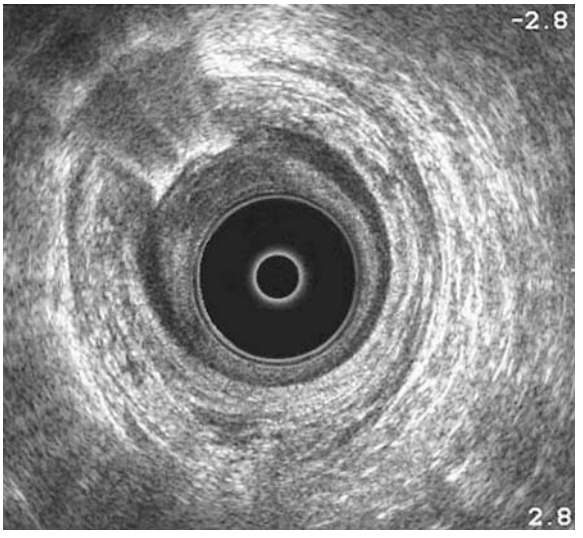

c

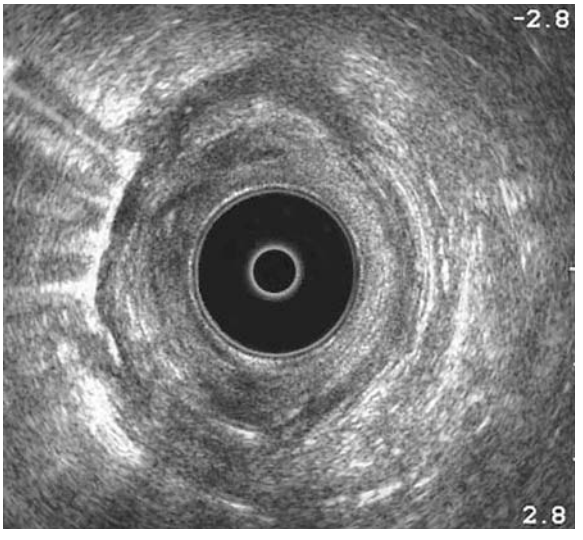

d

Case V.10. A 55-year-old man complaining of rectal pain and perianal purulent discharge from an external orifice at the 11 o'clock position. Preliminary endoanal ultrasonography (EAUS) scan at mid anal canal level reveals irregular thickening in the right lateral intersphincteric plane with a hypoechoic area containing air (hyperechoic spet) at the 11 o'clock position (**a**). After peroxide injection, the EAUS scan shows immediate communication with the area at the 11 o'clock position and through the internal anal sphincter with the anal lumen (**b**). Fistula extends anteriorly (**c**) and posteriorly (**d**) into the intersphincteric plane (horseshoe intersphincteric fistula)

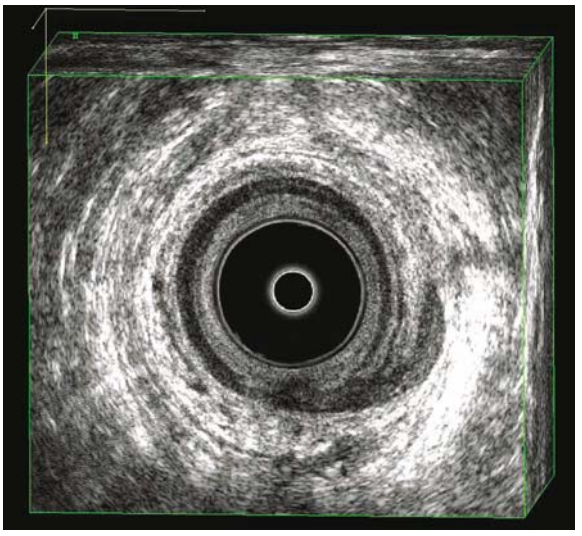

a

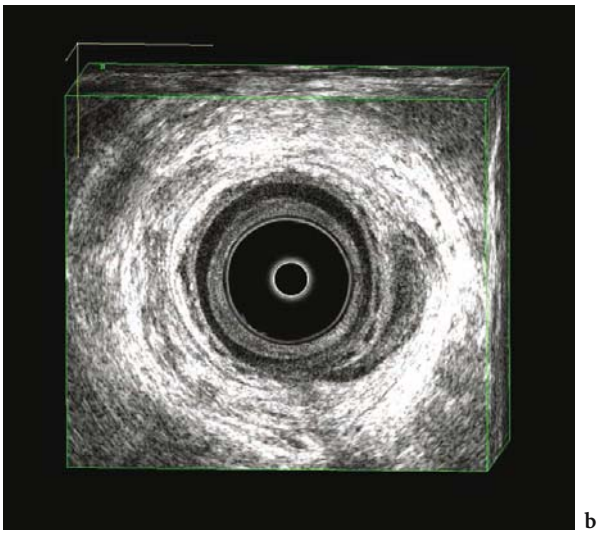

b

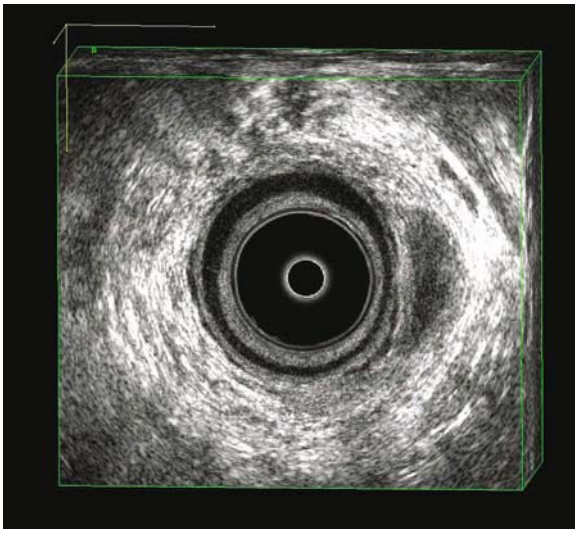

c

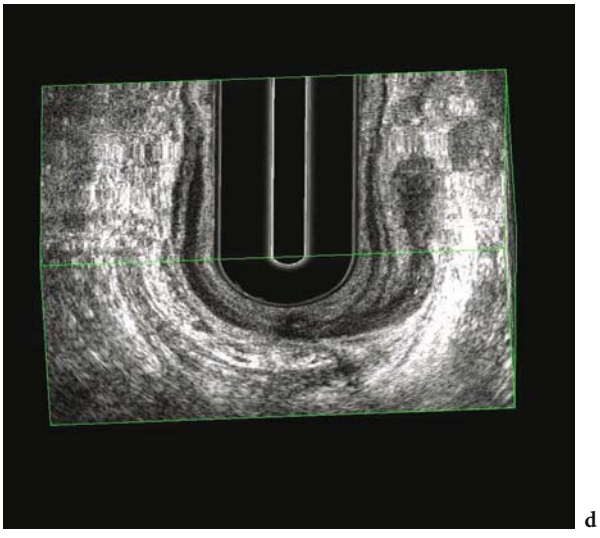

d

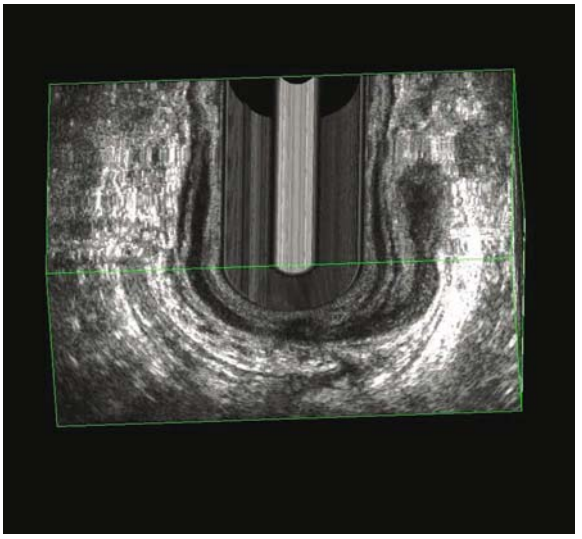

e

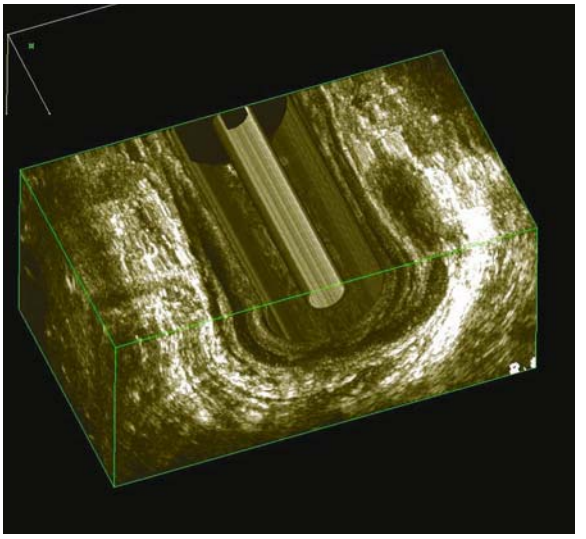

f

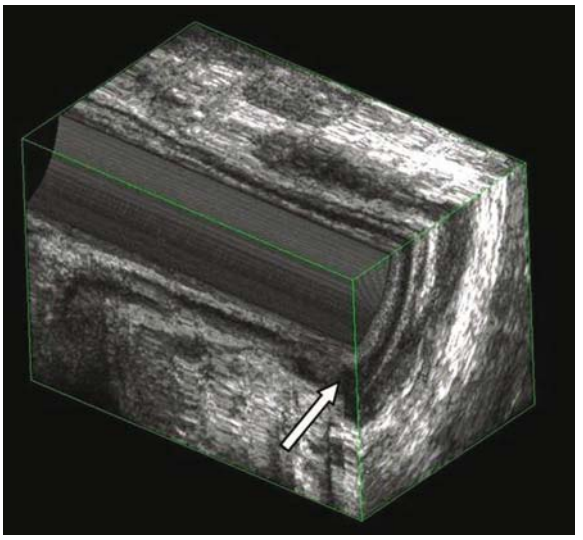

g

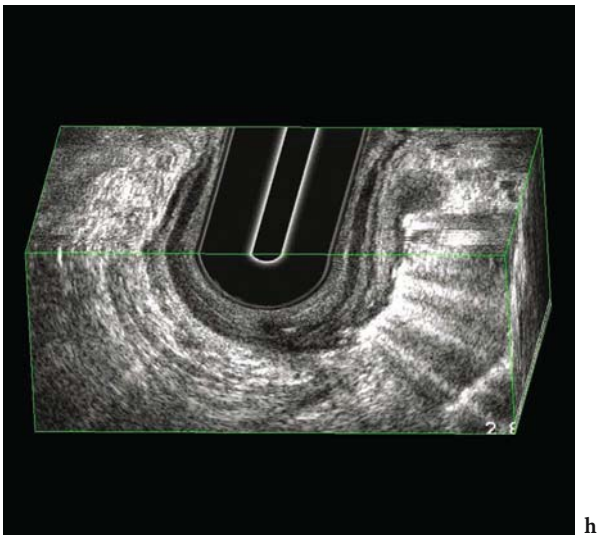

h

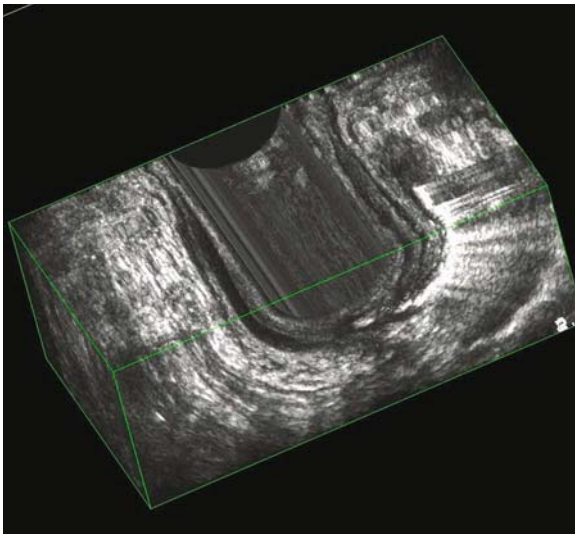

i

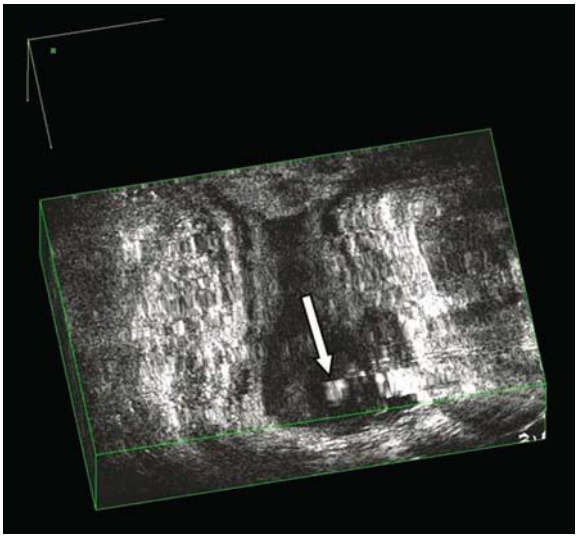

l

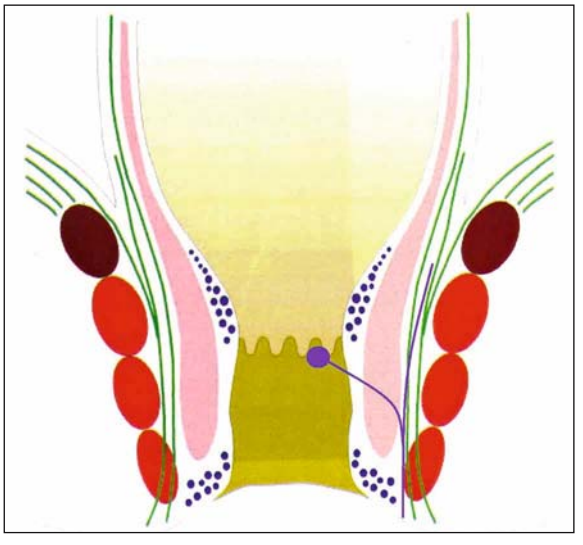

m

Case V.11. A 34-year-old woman complaining of recurrent perianal purulent discharge. Physical examination reveals a cutaneous opening at the 6 o'clock position. At mid anal canal level, three-dimensional reconstruction in the axial plane reveals a hypoechoic intersphincteric tract with an appearance of internal sphincter defect at the 6 o'clock position (**a**) (second endosonographic criteria for the site of an internal opening according to Cho [17]). The fistula also tracks upward and laterally into the intersphincteric plane (**b**, **c**). Reconstruction in the coronal plane confirms an intersphincteric fistula, with the internal opening at the 6 o'clock position, extending upward and laterally within the longitudinal layer (**d**). The tract causes widening and distortion of the intersphincteric plane without traversing the external sphincter. Volume render mode (**e**, **f**). Reconstruction in the sagittal plane confirms the presence of the internal opening at the 6 o'clock position (*arrow*) (**g**). After administration of peroxide, endoanal ultrasonography scan shows immediate communication with the anal lumen below the level of the internal anal sphincter and the extent of the intersphincteric fistula (**h**). Volume render mode (**i**). Internal orifice (*arrow*) (**l**). Drawing in the axial plane shows extent of the intersphincteric fistula (**m**)

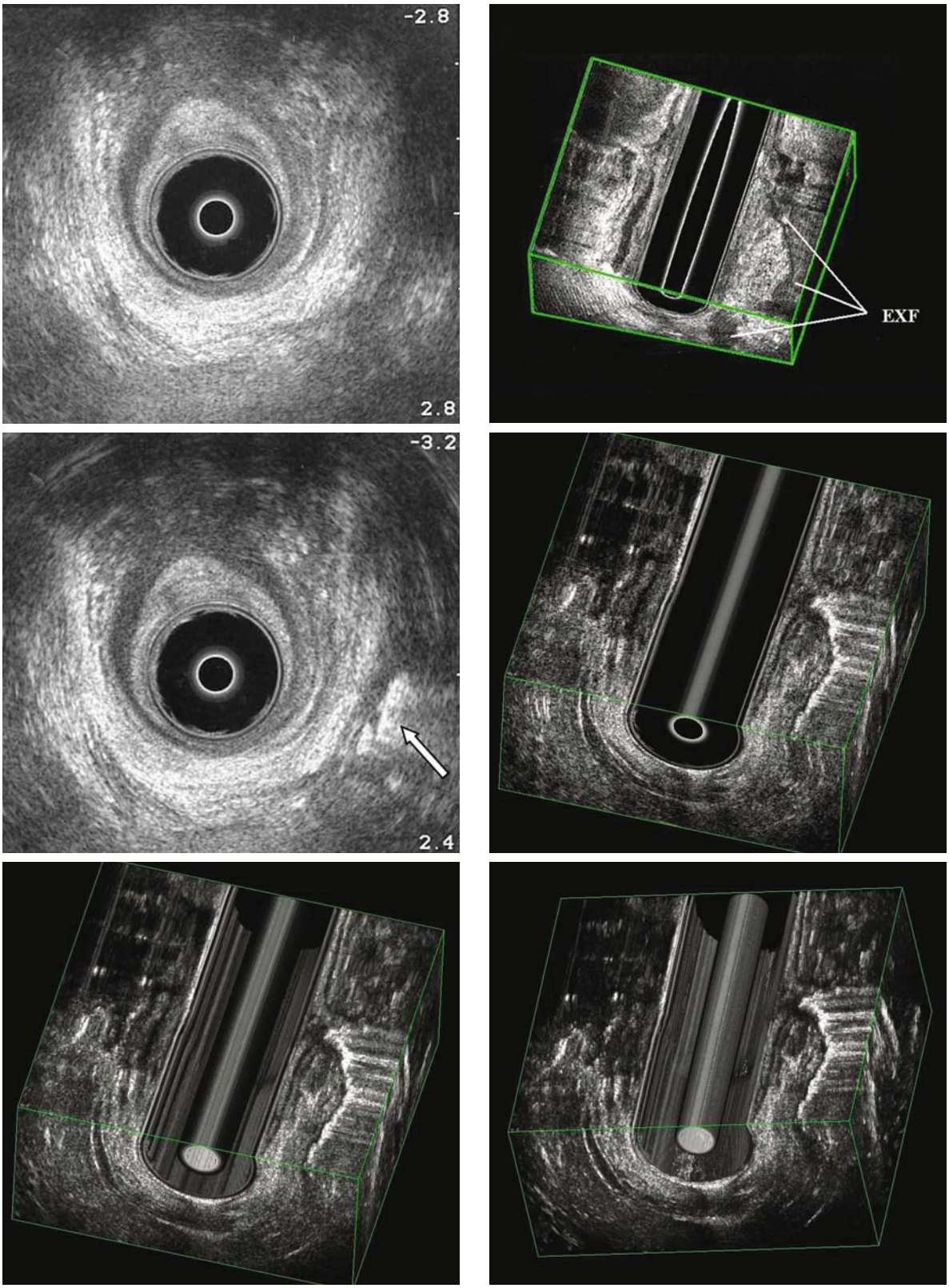

Case V.12. A 29-year-old man referred for recurrent perianal fistula. Axial endosonographic image shows a normal appearance of upper anal canal level (**a**). Three-dimensional (3-D) reconstruction in the coronal plane reveals a hypoechoic tract extending upward outside the internal and external sphincters (*EXF*, extrasphincteric fistula) (**b**). After peroxide injection, the axial scan shows the presence of bright echoes (*arrows*) at the 4 o'clock position at the upper anal canal level (**c**). 3-D hydrogen-peroxide-enhanced ultrasonography confirms an extrasphincteric fistula communicating with the rectal ampulla (**d**). Volume render mode (**e**, **f**)

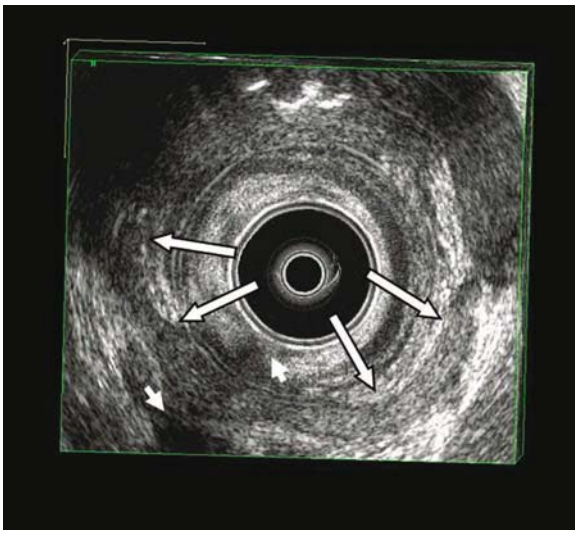

a

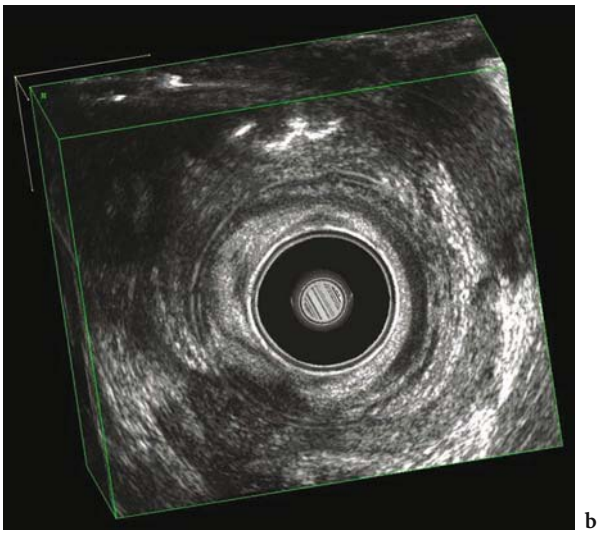

b

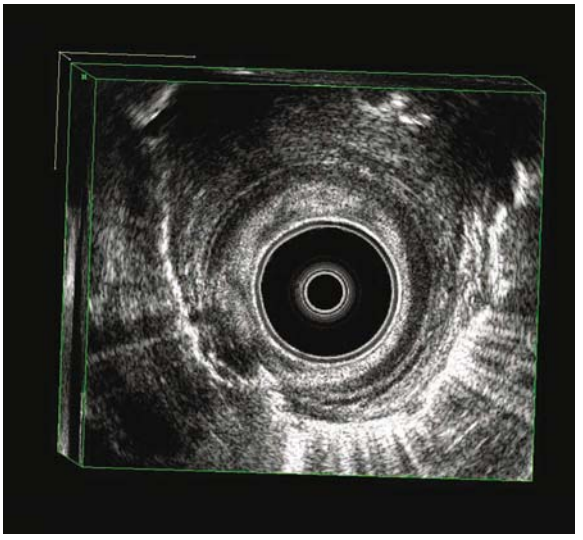

c

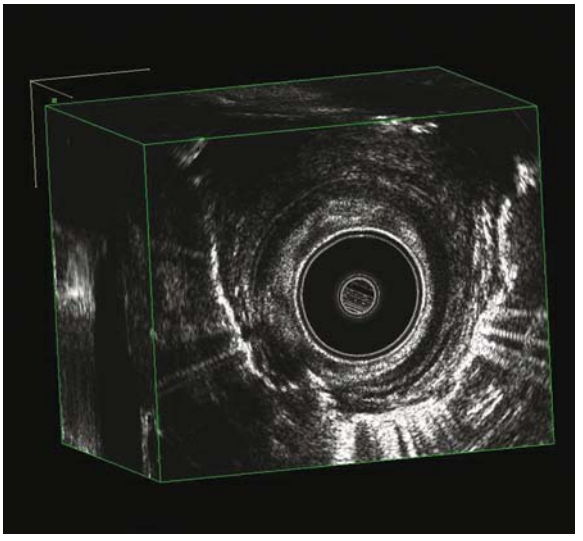

d

Case V.13. A 33-year-old man complaining of recurrent perianal fistula and purulent discharge from an external orifice at the 7 o'clock position. Three-dimensional endoanal ultrasonography (EAUS) scan at mid anal canal level shows a posterior hypoechoic tract extending through the internal and external sphincters (*small arrows*) and an irregular thickening in the right and left lateral intersphincteric plane (*large arrows*) (**a**). Volume render mode (**b**). After peroxide injection, the EAUS scan shows immediate communication through the internal sphincter into the anal lumen, with horseshoe extension into the intersphincteric plane (**c**). Volume render mode confirms the presence of a posterior transsphincteric fistula, with internal opening at the 7 o'clock position and secondary horseshoe intersphincteric extension (**d**)

a

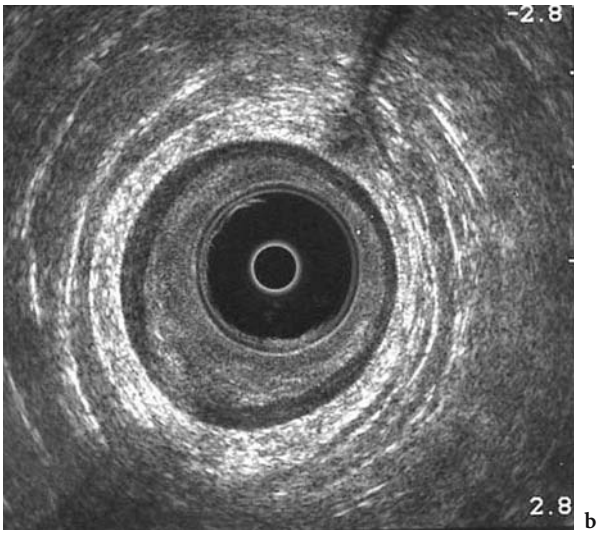

b

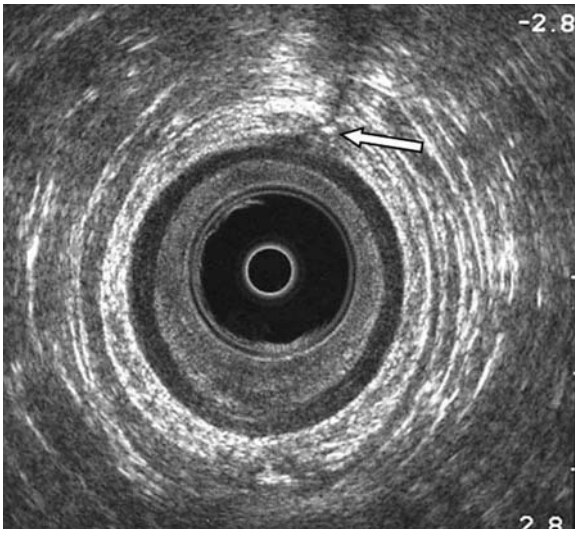

c

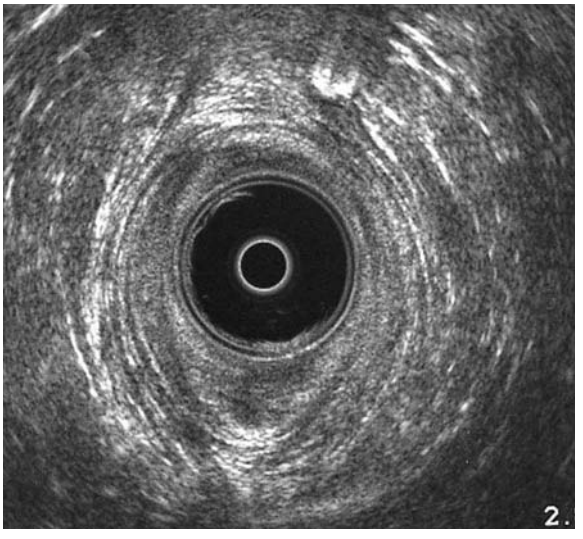

d

Case V.14. A 27-year-old woman referred for recurrent perianal fistula. Physical examination reveals a cutaneous scar at the 2 o'clock position where the external fistulous opening was previously located (**a**). Preliminary endoanal ultrasonography (EAUS) scan shows an anterior hypoechoic tract extending through the internal and external sphincters (**b**). After probing into the center of the cutaneous scar, the skin is easily broken and the peroxide injected into the external opening. The EAUS scans show immediate communication with the transsphincteric tract (**c**, **d**)

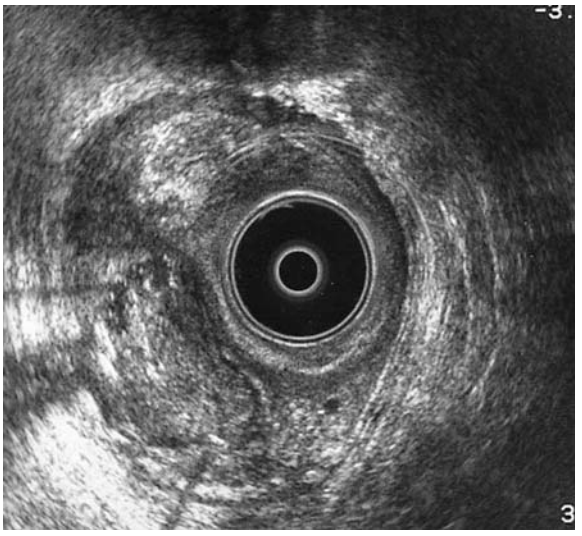

a

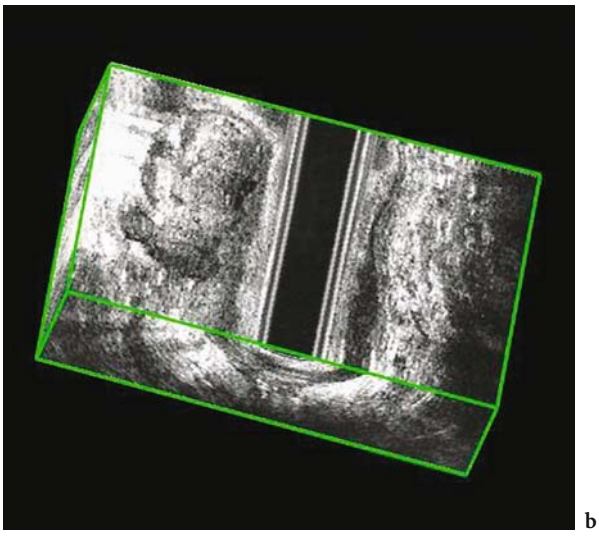

b

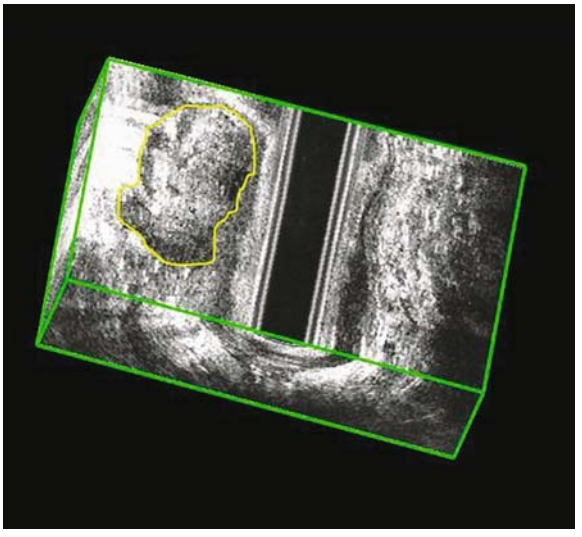

c

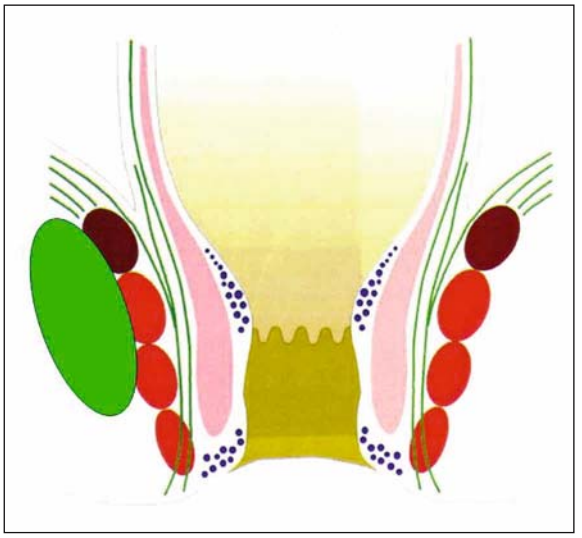

d

Case V.15. A 35-year-old man complaining of perirectal pain. Digital rectal examination reveals a right lateral tender mass at 2 cm from the anal verge. Axial endosonographic image of mid anal canal level reveals a large dishomogeneous area in the right lateral ischioanal space (**a**). Three-dimensional reconstruction in the coronal plane confirms the presence of a chronic ischioanal abscess (**b, c**). Drawing in the axial plane (**d**). The patient underwent drainage through the ischioanal space

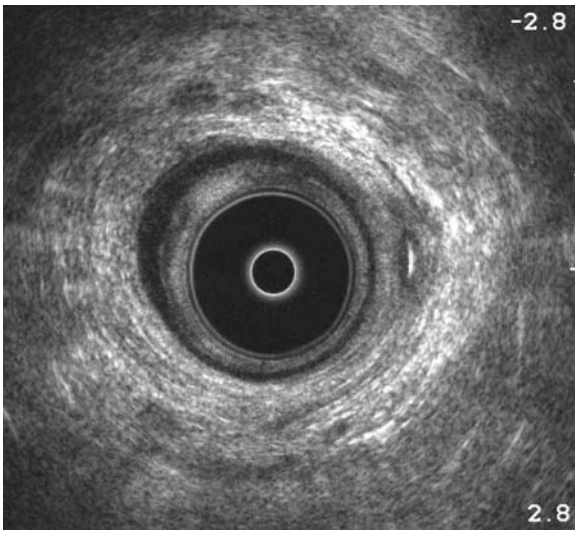

a

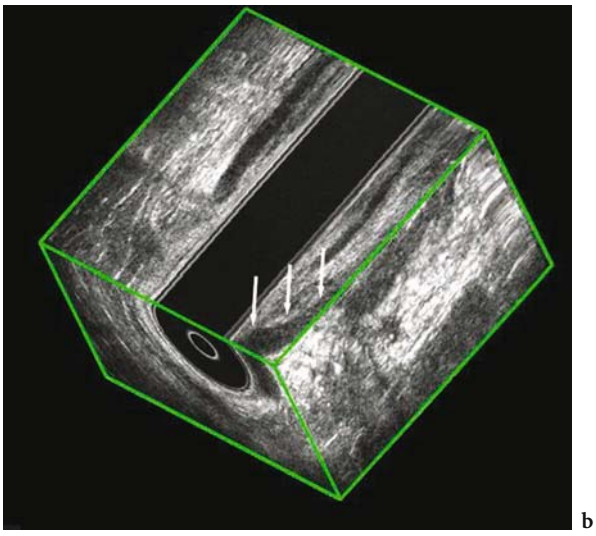

b

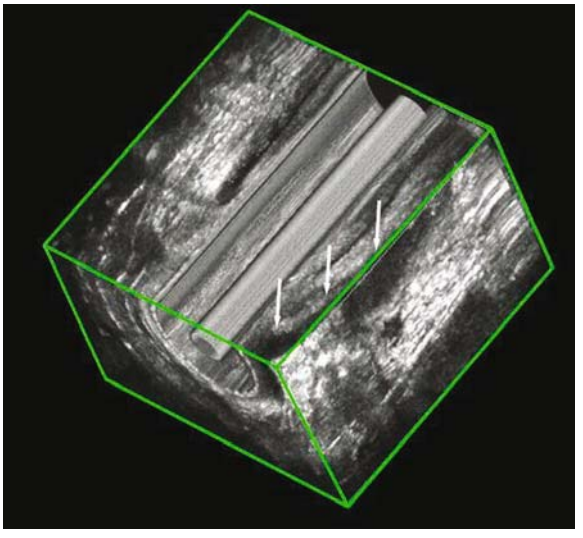

c

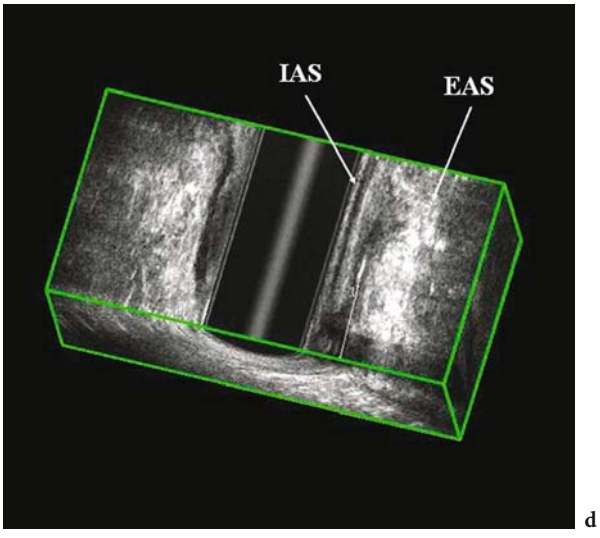

d

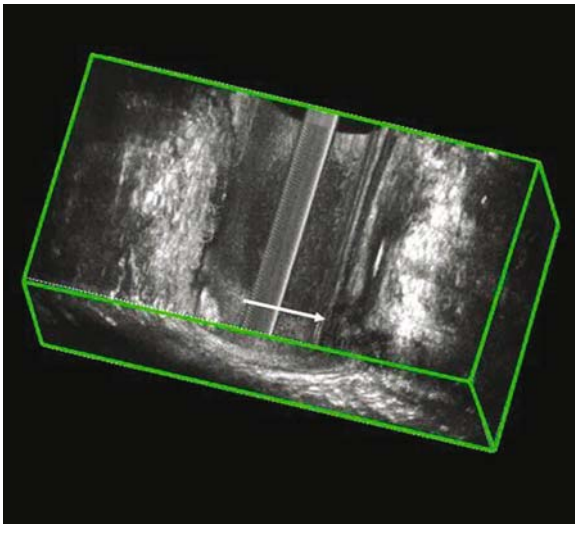

e

Case V.16. A 34-year-old woman complaining of perianal purulent discharge from the anus. Axial endosonographic image of mid anal canal level reveals in the intersphincteric zone at the 3 o'clock position a hypoechoic area with a bright echo inside for the presence of air (**a**). Three-dimensional ultrasonography scans show a simple intersphincteric fistula that extends from the lower anal canal to the middle anal canal (*arrows*) (**b–d**). Volume render mode demonstrates a direct communication (internal opening) with the lower part of the anal canal (*arrow*) (**e**). *IAS*: internal anal sphincter, *EAS*: external anal sphincter

a

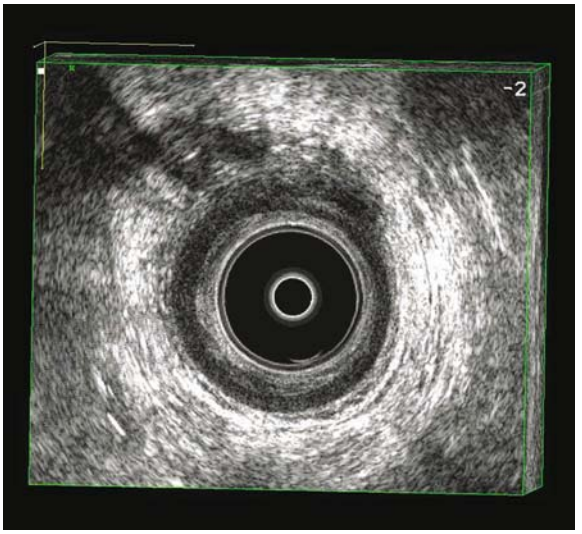

b

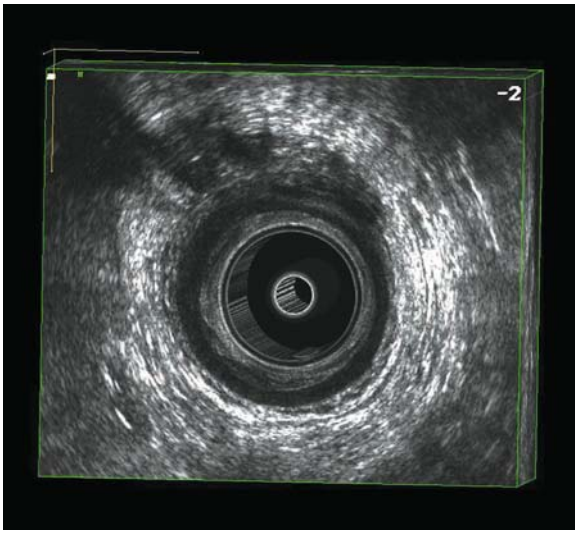

c

d

Case V.17. A 36-year-old woman complaining of perianal purulent discharge. Physical examination reveals a cutaneous opening at the 11 o'clock position (**a**). Axial endosonographic image at mid anal canal level shows an anterior hypoechoic tract extending through the external sphincter, which contacts the internal sphincter at the 12 o'clock position (transsphincteric fistula) (**b**). Volume render mode (**c**). The patient underwent a laid-open procedure (**d**)

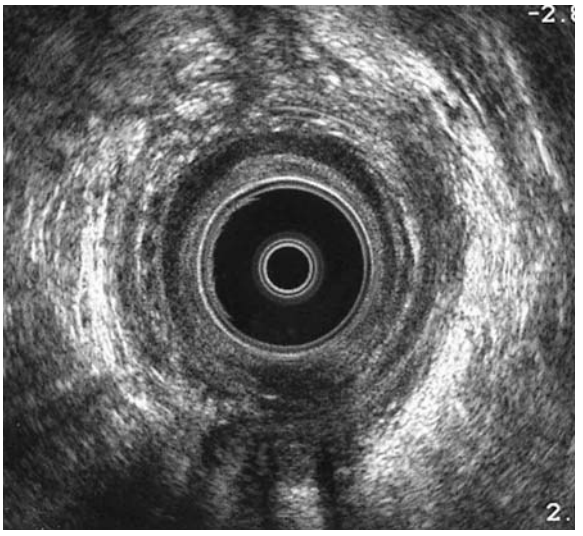

a

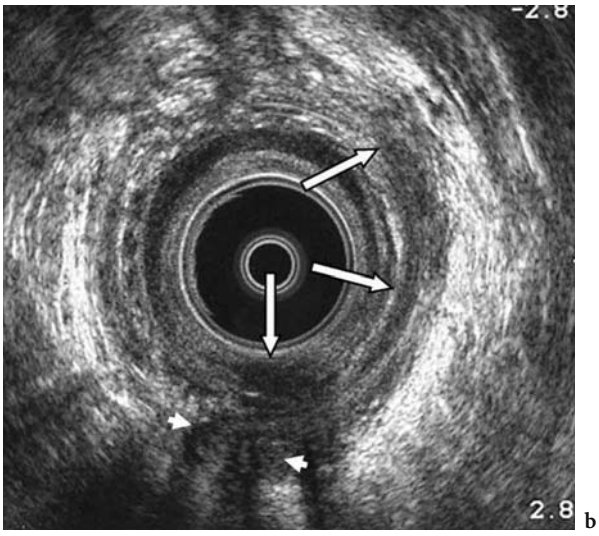

b

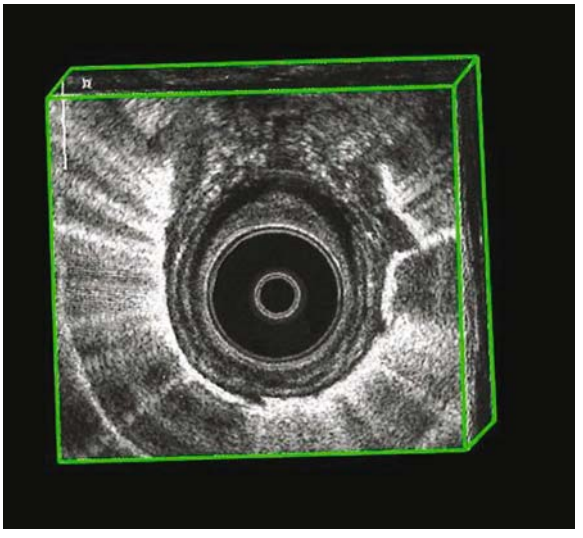

c

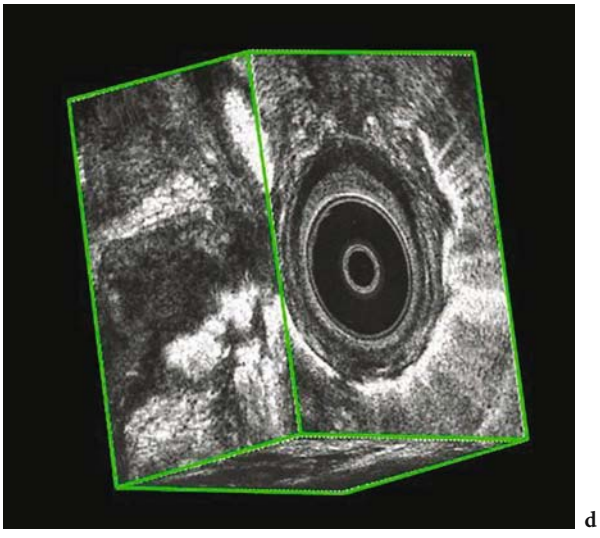

d

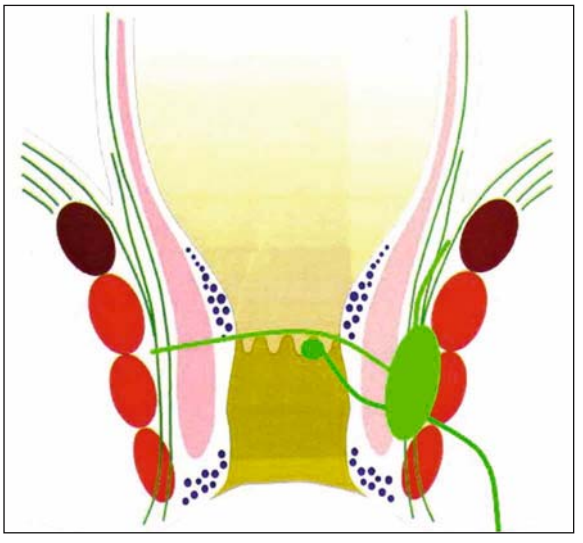

e

Case V.18. A 53-year-old man complaining of fever and purulent discharge from an external orifice at the 6 o'clock position. Axial endoanal ultrasonography (EAUS) scans at mid anal canal level show a posterior, large, intersphincteric hypoechoic area (acute intersphincteric abscess) with a primary tract (*small arrows*) extending from this area through the external sphincter (transsphincteric fistula) and a secondary tract extending through the left side of the intersphincteric plane (*large arrows*) (**a**, **b**). After peroxide injection, the EAUS scan reveals an horseshoe extension into the intersphincteric plane (**c**). Three-dimensional reconstruction on the sagittal plane shows upward extension of the horseshoe secondary tract (**d**). Drawing in the axial plane shows extent of the abscess and fistulas (**e**)

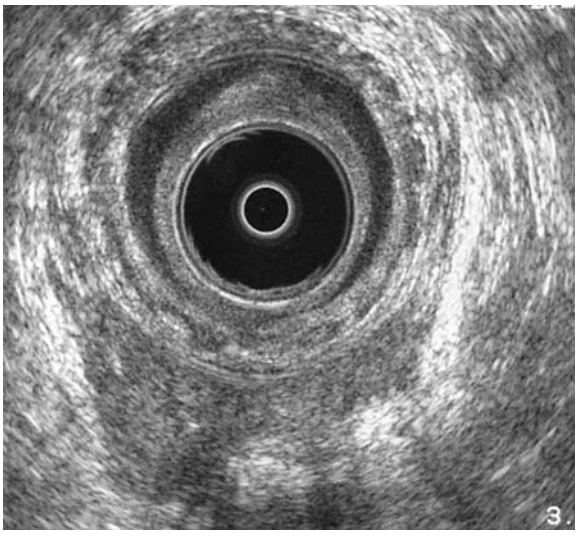

a

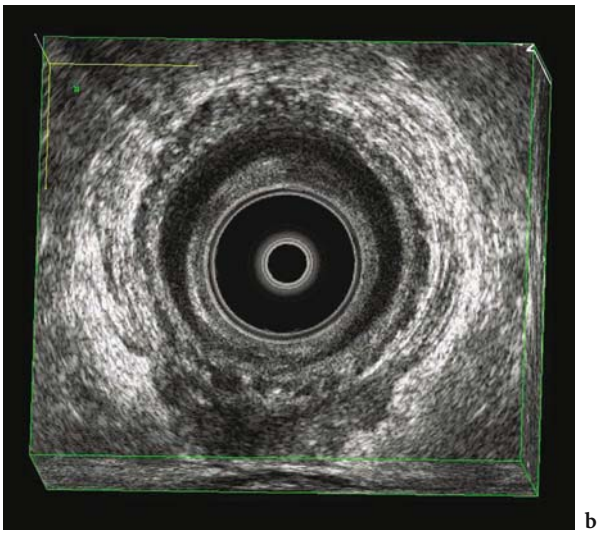

b

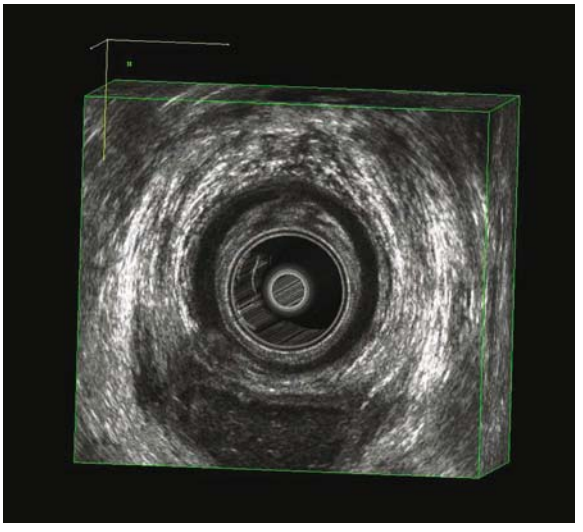

c

Case V.19. A 58-year-old man complaining of fever and perirectal pain. Digital rectal examination reveals a posterior tender mass at the dentate line level 2 cm from the anal verge. Axial endosonographic image of mid anal canal level reveals a large hypoechoic area in the posterior intersphincteric zone (**a**). Three-dimensional endoanal ultrasonography scan confirms the presence of an acute posterior intersphincteric abscess (**b**). Volume render mode (**c**)

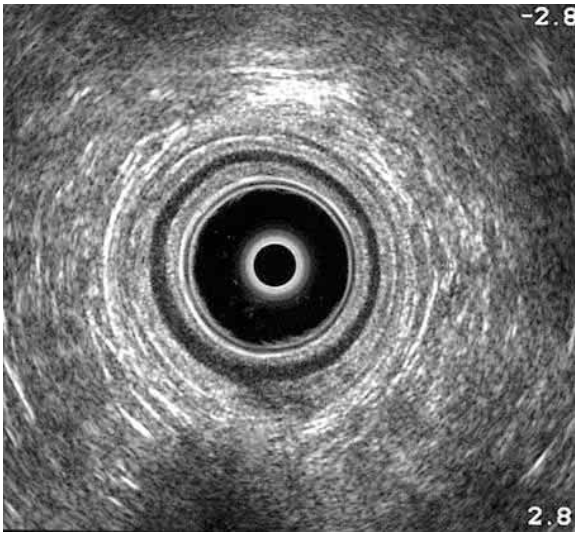

a

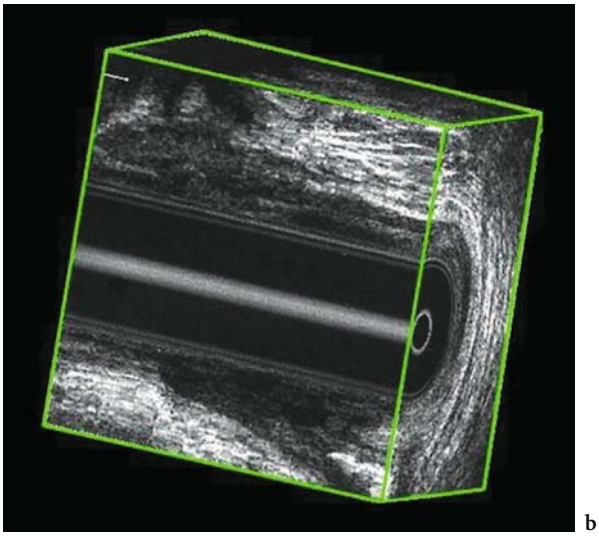

b

Case V.20. A 37-year-old woman complaining of perianal pain. Axial endosonographic image of mid anal canal level reveals a hypoechoic area in the intersphincteric zone at the 6 o'clock position (**a**). Sagittal view from a three-dimensional data set shows a low intersphincteric tract (**b**). The patient underwent a laid-open procedure

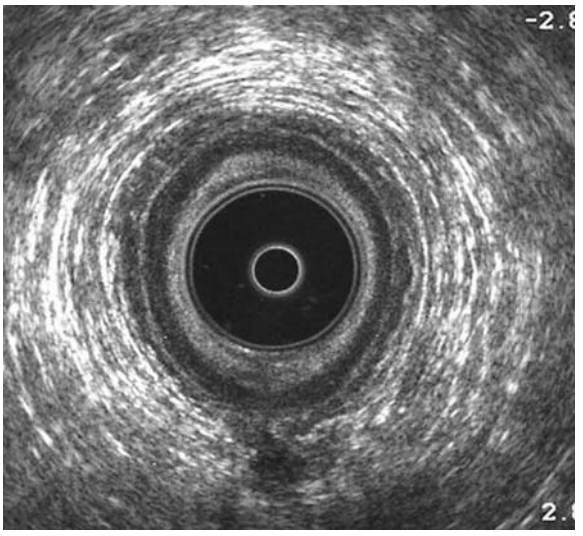

a

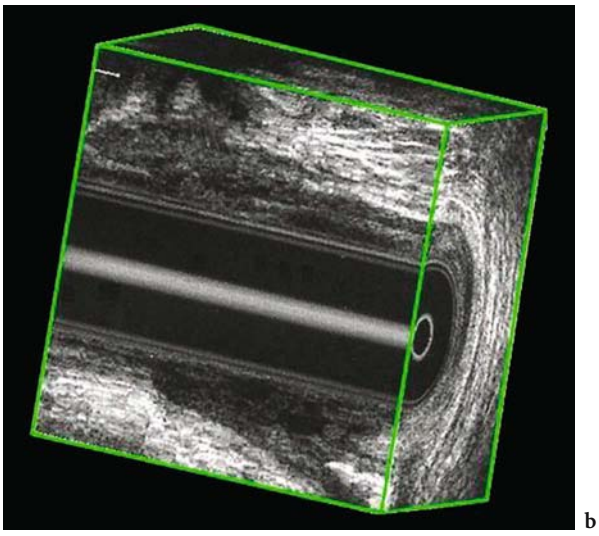

b

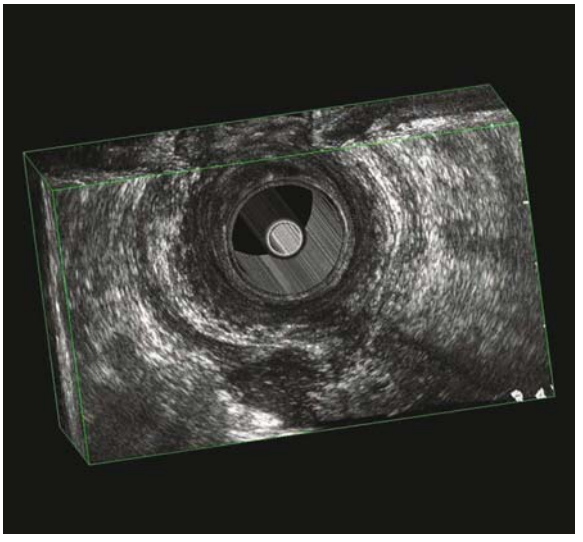

c

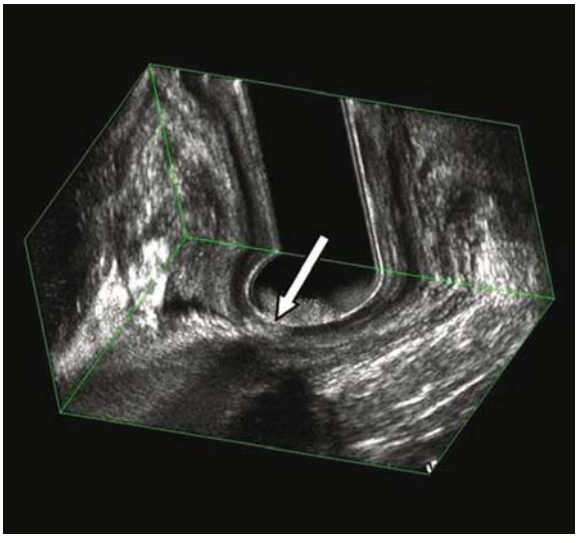

d

Case V.21. A 43-year-old man complaining of recurrent perianal purulent discharge. Physical examination reveals a cutaneous opening at the 6 o'clock position. Axial endosonographic image at mid anal canal level shows a posterior hypoechoic tract extending through the external sphincter, which contacts the internal sphincter at the 6 o'clock position (third endosonographic criteria for the site of an internal opening according to Cho [17]) (**a**). Sagittal view from a three-dimensional data set confirming the presence of a low transsphincteric fistula that traverses only the distal third of the external sphincter (**b**). Volume render mode (**c**, **d**). The internal opening is located at the 6 o'clock position (*arrow*). After demonstration of the limited involvement of the external sphincter, the patient underwent a fistulotomy, with no loss of continence

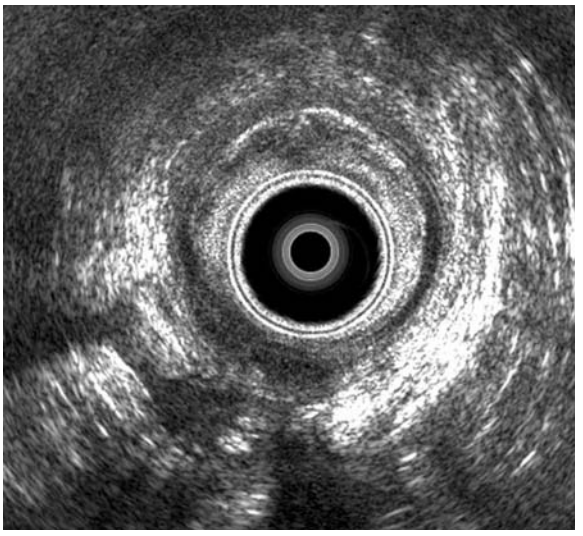

a

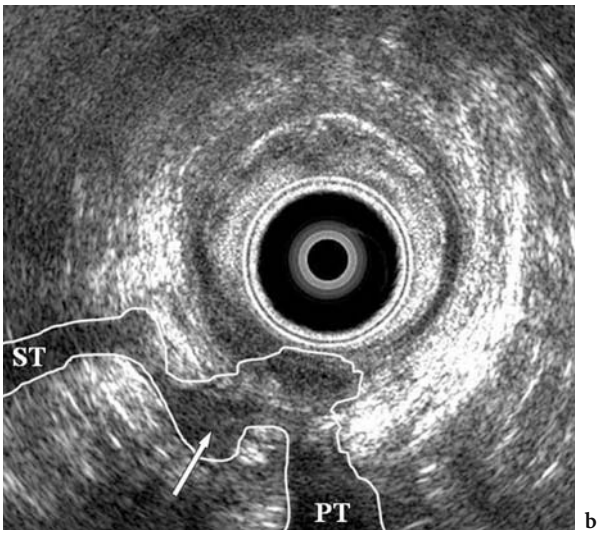

b

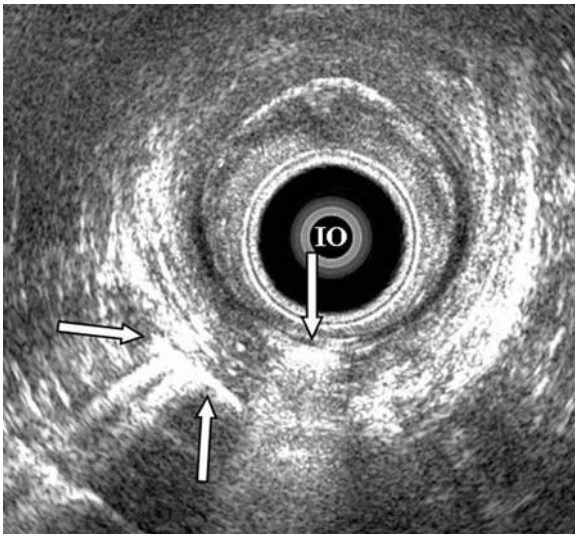

c

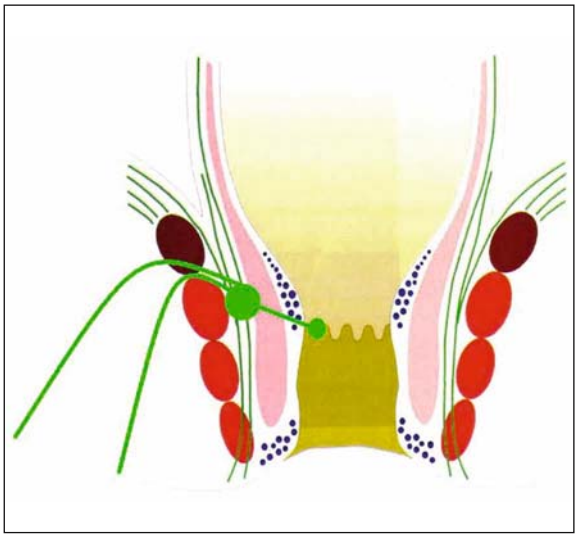

d

Case V.22. A 28-year-old woman referred for recurrent perianal fistulas. Physical examination reveals two external openings at the 6 and 9 o'clock positions, respectively. Axial endoanal ultrasonography (EAUS) scan shows an intersphincteric hypoechoic area (acute intersphincteric abscess) at the 6 o'clock position (*arrow*), with a primary tract (*PT*) extending posteriorly from this area through the puborectal muscle (suprasphincteric fistula) and a secondary tract (*ST*) extending in the right side and traversing the puborectal muscle at the 9 o'clock position (**a**, **b**). After injection of peroxide from the external opening at the 6 o'clock position, the EAUS scan reveals an immediate communication with the anal lumen (*IO* internal opening) (**c**). Drawing in the axial plane shows extent of the abscess and fistulas (**d**)

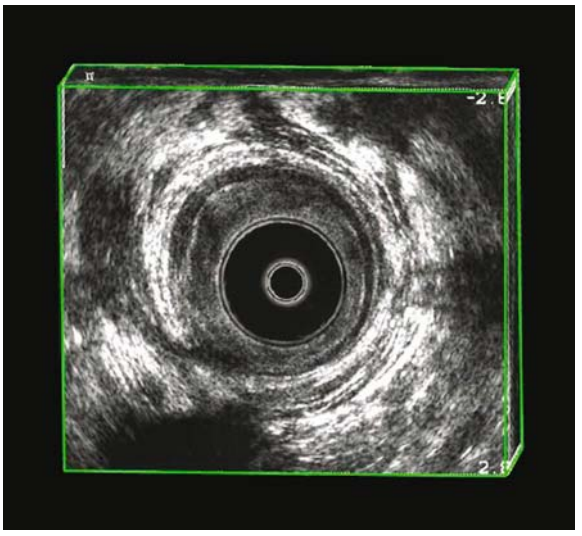

a

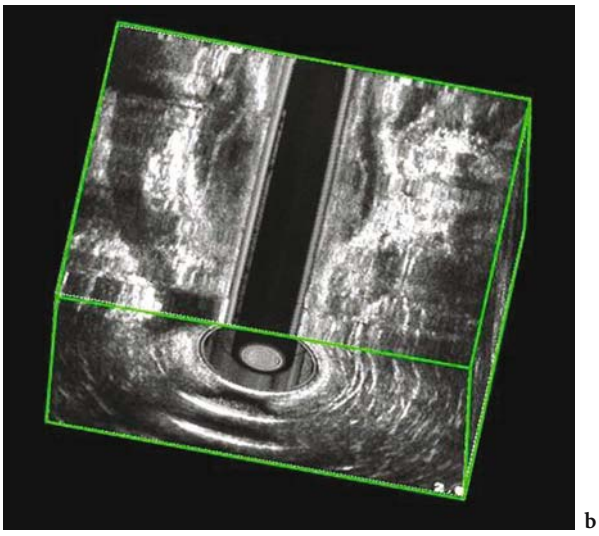

b

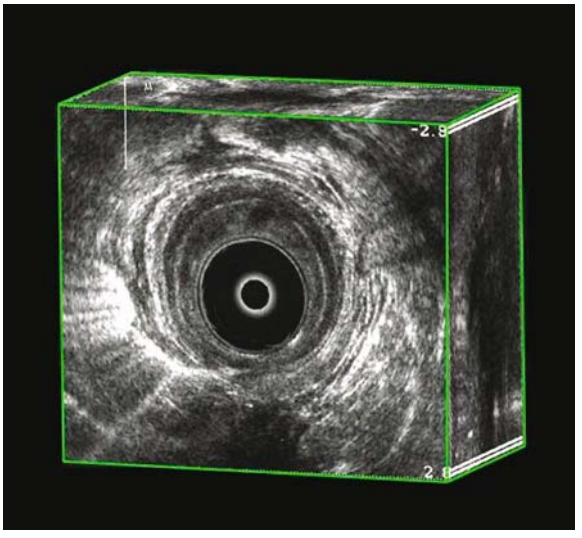

c

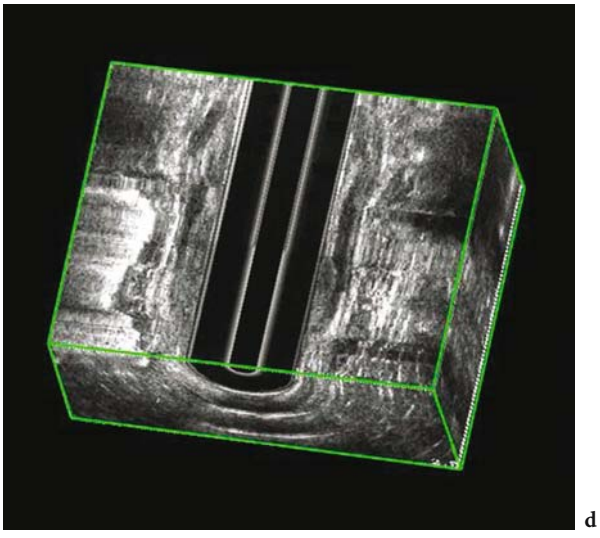

d

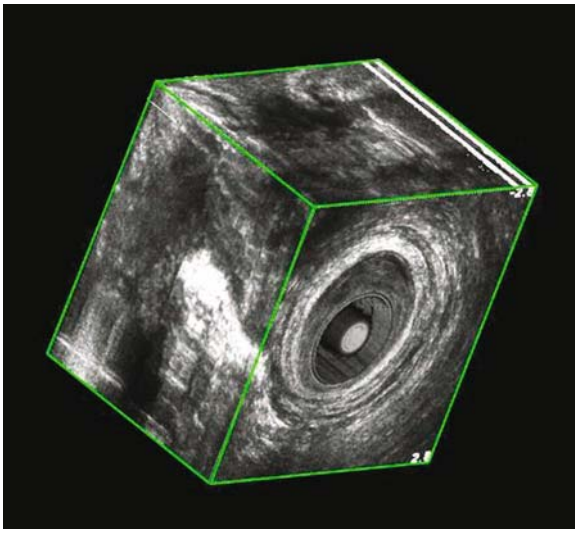

e

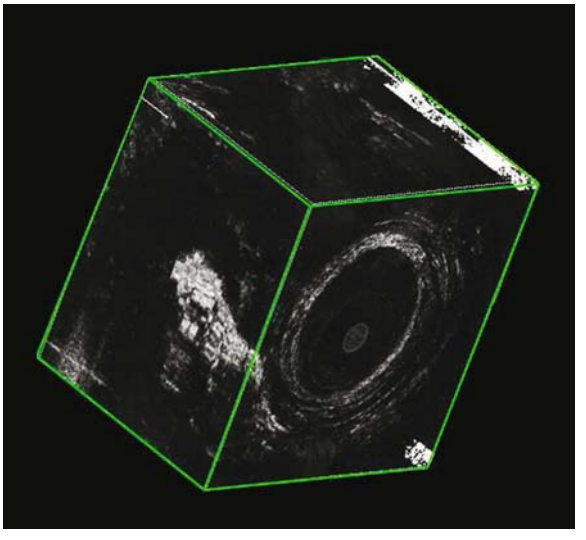

f

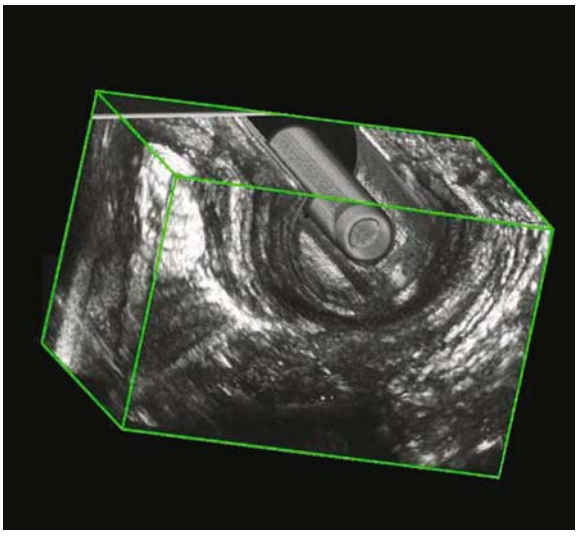

g

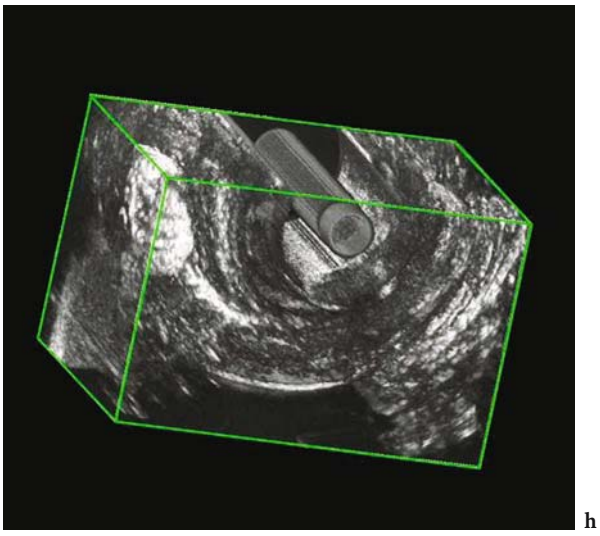

h

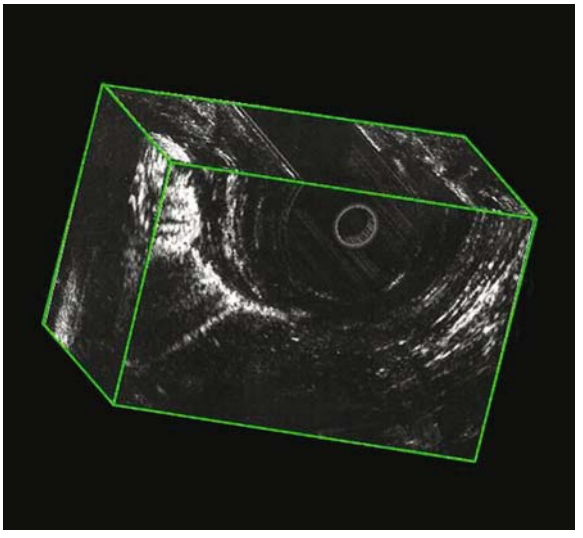

i

Case V.23. A 26-year-old man with recurrent perianal Crohn's disease. Axial endosonographic image of mid anal canal level reveals a hypoechoic area into the right ischiorectal fossa (acute abscess) with a primary tract extending from this area and traversing the external and internal sphincter at the 6 o'clock position (transsphincteric fistula) (**a**). Three-dimensional reconstruction on the coronal plane shows upward extension of the ischiorectal abscess (**b**). After peroxide injection through a cutaneous orifice at the 9 o'clock position (right lateral side) endoanal ultrasonography scans with volume render mode confirm the presence of an acute ischiorectal abscess (**c-f**) with a transsphincteric fistula (**g-i**)

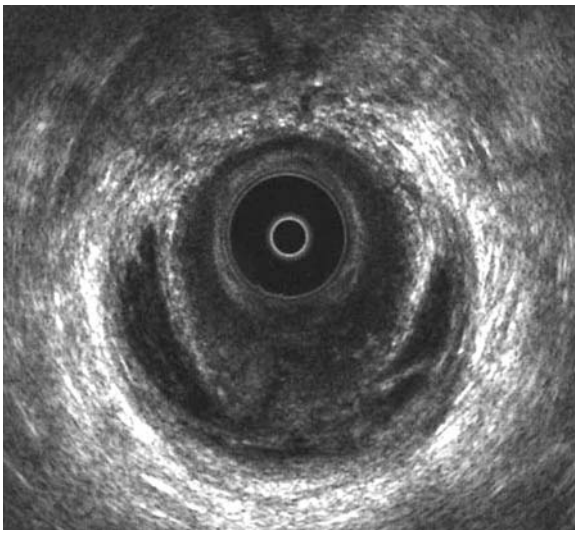

a

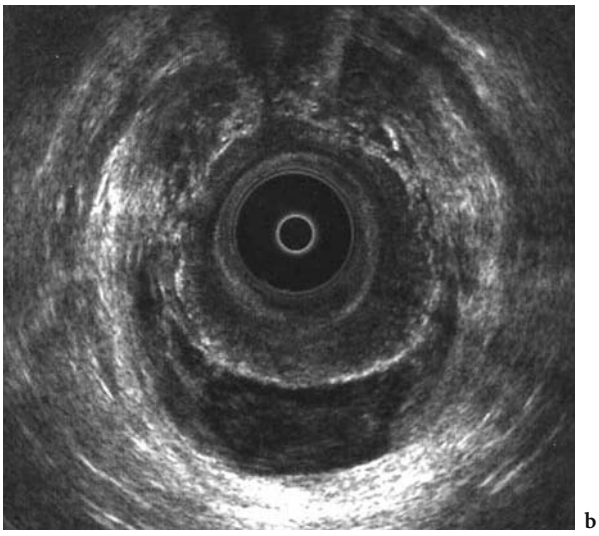

b

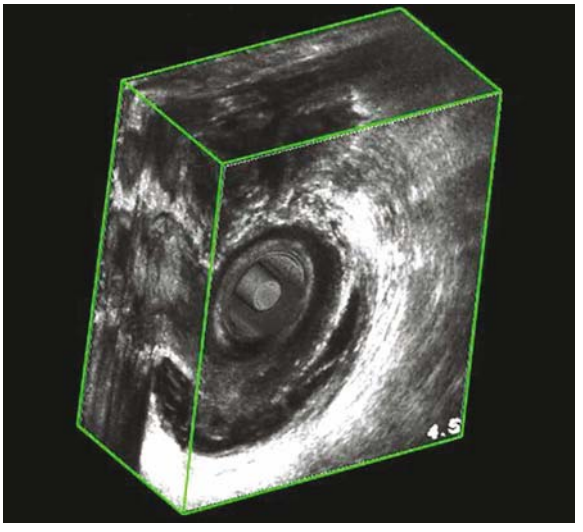

c

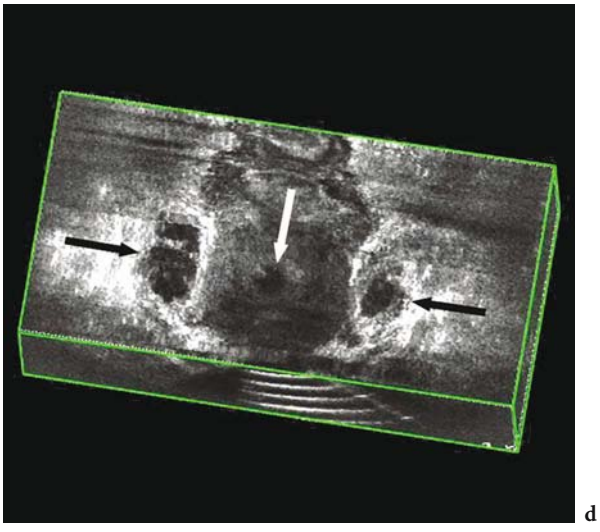

d

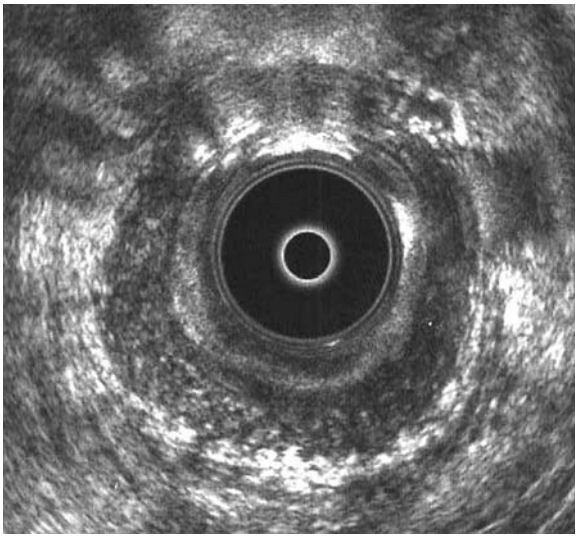

e

Case V.24. A 38-year-old man complaining of fever and perirectal pain. Digital rectal examination reveals a posterior tender mass at the puborectalis level. Axial endosonographic images of upper anal canal level reveal a large horseshoe hypoechoic area in the posterior intersphincteric zone (**a**, **b**). Three-dimensional endoanal ultrasonography scans with volume render mode confirm the presence of an acute horseshoe intersphincteric abscess (**c**) and demonstrate the internal orifice (**d**) (*white arrow*: internal opening; *black arrows*: horseshoe abscess). The patient underwent immediate drainage through the intersphincteric space, as confirmed by postoperative ultrasonography (**e**)